THE JOURNAL OF BIOLOGICAL CHEMISTRY VOL. 287, NO. 24, pp. 20674–20688, June 8, 2012

Interaction with Caveolin-1 Modulates G Protein Coupling of Mouse β_3-Adrenoceptor*[S]

Received for publication, July 11, 2011, and in revised form, April 19, 2012 Published, JBC Papers in Press, April 25, 2012, DOI 10.1074/jbc.M111.280651

Masaaki Sato[‡§], Dana S. Hutchinson[‡1], Michelle L. Halls[‡1], Sebastian G. B. Furness[‡], Tore Bengtsson[§], Bronwyn A. Evans[‡2], and Roger J. Summers[‡]

From [‡]Drug Discovery Biology, Monash Institute of Pharmaceutical Sciences and the Department of Pharmacology, Monash University, Parkville, Victoria 3052, Australia and the [§]Department of Physiology, The Wenner-Gren Institute, Arrhenius Laboratories F3, Stockholm University, SE-106 91 Stockholm, Sweden

Background: Caveolins affect signaling by G protein-coupled receptors (GPCRs).
Results: Interaction between β_{3a}-adrenoceptors and caveolin-1 facilitates G_s-mediated responses but prevents the receptor from coupling to inhibitory $G_{i/o}$ proteins.
Conclusion: Association of the β_{3a}-adrenoreceptor with caveolin-1 is important in determining the selectivity and efficiency of G protein coupling and signaling.
Significance: We demonstrate the functional impact of a GPCR-caveolin association.

Caveolins act as scaffold proteins in multiprotein complexes and have been implicated in signaling by G protein-coupled receptors. Studies using knock-out mice suggest that β_3-adrenoceptor (β_3-AR) signaling is dependent on caveolin-1; however, it is not known whether caveolin-1 is associated with the β_3-AR or solely with downstream signaling proteins. We have addressed this question by examining the impact of membrane rafts and caveolin-1 on the differential signaling of mouse β_{3a}- and β_{3b}-AR isoforms that diverge at the distal C terminus. Only the β_{3b}-AR promotes pertussis toxin (PTX)-sensitive cAMP accumulation. When cells expressing the β_{3a}-AR were treated with filipin III to disrupt membrane rafts or transfected with caveolin-1 siRNA, the cyclic AMP response to the β_3-AR agonist CL316243 became PTX-sensitive, suggesting $G\alpha_{i/o}$ coupling. The β_{3a}-AR C terminus, SP^{384}PLNRF^{389}DGY^{392}EGARPF^{398}PT, resembles a caveolin interaction motif. Mutant β_{3a}-ARs (F389A/Y392A/F398A or P384S/F389A) promoted PTX-sensitive cAMP responses, and *in situ* proximity assays demonstrated an association between caveolin-1 and the wild type β_{3a}-AR but not the mutant receptors. In membrane preparations, the β_{3b}-AR activated $G\alpha_o$ and mediated PTX-sensitive cAMP responses, whereas the β_{3a}-AR did not activate $G\alpha_{i/o}$ proteins. The endogenous β_{3a}-AR displayed $G\alpha_{i/o}$ coupling in brown adipocytes from caveolin-1 knock-out mice or in wild type adipocytes treated with filipin III. Our studies indicate that interaction of the β_{3a}-AR with caveolin inhibits coupling to $G\alpha_{i/o}$ proteins and suggest that signaling is modulated by a raft-enriched complex containing the β_{3a}-AR, caveolin-1, $G\alpha_s$, and adenylyl cyclase.

The plasma membrane is not a random or uniform array of lipids and proteins but instead has physical heterogeneity as well as higher order structures that are critical to the functioning of receptors, ion channels, and signaling proteins. Membrane rafts, or lipid rafts, are liquid-ordered lipid domains of 5–10 nm that are enriched in cholesterol and sphingolipids (1, 2). Rafts display reduced lateral diffusion relative to the liquid-disordered phase, providing nucleation sites for further membrane organization to produce larger structures of 50–150 nm. These higher order structures are enriched in multiprotein complexes, acting as signaling platforms that govern association between receptors and effector proteins (reviewed in Ref. 3). Caveolae represent a subset of membrane rafts that have a distinctive membrane structure delineated by the presence of caveolin proteins as well as the protein cavin (4, 5). Caveolin-1, -2, and -3 consist of a cytoplasmic N terminus, a 21-amino acid hairpin structure that inserts into the cell membrane, and a cytoplasmic C terminus with three palmitoylation sites. Caveolins interact with signaling proteins via a conserved scaffolding domain (for example, amino acids 82–101 of caveolin-1). Caveolae are thought to contain 100–200 caveolin molecules (6); however, caveolins may form smaller noncaveolar oligomers of at least 15 molecules that have been termed caveolin scaffolds (7). Noncaveolar caveolins may also modulate signaling (4), for example by growth factor receptors (8) and G protein-coupled receptors (GPCRs)[3] (9).

The three β-adrenoreceptor subtypes (β-ARs) are highly conserved GPCRs that share common determinants for cou-

* This work was supported by National Health and Medical Research Council of Australia Program Grant 519461 (to P. M. Sexton, A. Christopoulos, and R. J.), National Health and Medical Research Council of Australia Career Development Award 545952 (to D. S. H.), National Health and Medical Research Council of Australia C. J. Martin Fellowship 519581 (to M. L. H.), and by Australian Research Council Linkage International Fellowship LX0989791 (to M. S.).

[S] This article contains supplemental Tables S1–S3.

[1] Both authors contributed equally to this work.

[2] To whom correspondence should be addressed: Drug Discovery Biology, Monash Institute of Pharmaceutical Sciences, Monash University, 399 Royal Parade, Parkville, Victoria 3052, Australia. Tel.: 61-3-9903-9086; E-mail: bronwyn.evans@monash.edu.

[3] The abbreviations used are: GPCR, G protein-coupled receptor; AC, adenylyl cyclase; β-AR, β-adrenoceptor; β_3-AR, β_3-adrenoceptor; BAT, brown adipose tissue; cav-1, caveolin-1; $G\alpha_s$, stimulatory guanine-nucleotide binding protein; $G\alpha_{i/o}$, inhibitory guanine nucleotide-binding protein; PTX, pertussis toxin; GTPγS, guanosine 5′-3-*O*-(thio)triphosphate; IBMX, 3-isobutyl-1-methylxanthine; ANOVA, analysis of variance; fsk, forskolin.

pling to the α subunit of the stimulatory guanine nucleotide-binding protein ($G\alpha_s$); however, functional diversity is generated by sequence-specific protein-protein interactions and by differential enrichment in membrane domains. For example, interaction of the β_2-AR with inhibitory guanine nucleotide-binding proteins ($G\alpha_{i/o}$) is dependent on the presence of a functional type 1 PSD-95/*Drosophila* Discs Large/ZO-1 (PDZ) docking site at the receptor C terminus (DSLL) (10), whereas the β_1-AR C-terminal PDZ motif (ESKV) inhibits receptor internalization and $G\alpha_i$ coupling (11). The signaling properties of the β_2-AR are clearly regulated by partitioning in membrane rafts or in caveolae (12). In cardiac myocytes, disruption of caveolae has no effect on the inotropic response to β_1-AR stimulation, although it significantly enhances β_2-AR-mediated Ca^{2+} transients and L-type Ca^{2+} channel currents (13, 14).

Although no studies to date have reported localization of the β_3-AR in membrane rafts or caveolae, there is firm evidence that caveolin-1 regulates β_3-AR signaling in adipocytes. In both white and brown adipocytes, β_3-ARs stimulate the $G\alpha_s$/adenylyl cyclase/protein kinase A (PKA) pathway, promoting breakdown of fat (lipolysis) via phosphorylation of perilipin and hormone-sensitive lipase. Brown adipocytes also display β_3-AR-mediated thermogenesis via induction of the mitochondrial uncoupling protein UCP1. The role of caveolin-1 in both white and brown adipocytes has been examined using caveolin-$1^{-/-}$ mice. Stimulation of lipolysis by the β_3-AR selective agonist CL316243 is reduced substantially in white adipocytes isolated from caveolin-$1^{-/-}$ mice compared with wild type mice, due to disruption of a signaling complex that normally includes caveolin-1, the catalytic subunit of PKA and perilipin (15). A similar pattern is seen in differentiated 3T3-L1 adipocytes treated with caveolin-1 siRNA (16). In control cells, CL316243 promotes phosphorylation of perilipin, hormone-sensitive lipase, and also the phosphorylation, activation, and recruitment of phosphodiesterase 3B into complexes that contain caveolin-1, β_3-AR, and PKA regulatory subunit RII. Knockdown of caveolin-1 blocks the activation of PDE3B and its recruitment into plasma membrane signaling complexes. In brown adipose tissue from caveolin-$1^{-/-}$ mice, perilipin phosphorylation and the mobilization of triglycerides usually associated with fasting/cold exposure are substantially reduced (17). Upstream cAMP responses are also reduced, in part due to decreased adenylyl cyclase activity and β_3-AR abundance (18, 19). It cannot be determined from these studies, however, whether caveolin-1 is associated functionally with the β_3-AR itself or whether the diminished responses in knock-out mice are due solely to effects on downstream signaling, for example via PKA and perilipin.

We have been able to address this question by taking advantage of the distinct signaling properties of two mouse β_3-AR isoforms generated by alternative splicing (20, 21). The β_{3a}- and β_{3b}-AR isoforms differ only in their distal C-terminal tail, yet cAMP accumulation mediated by the β_{3b}-AR is increased following pretreatment of cells with pertussis toxin (PTX), whereas the β_{3a}-AR response is PTX-insensitive. Use of cell-permeable peptides corresponding to the unique β_{3a}- and β_{3b}-AR C termini demonstrated that the β_{3a}-AR C-terminal tail interacts with a distinct protein or signaling complex (22). We proposed that binding of proteins such as caveolin or other scaffolding proteins to the β_{3a}-AR C terminus may localize the receptor to membrane microdomains or intracellular compartments where it cannot couple to $G\alpha_{i/o}$.

We demonstrate here that when CHO-K1 cells expressing the β_{3a}-AR are treated with filipin III to disrupt membrane rafts, the cyclic AMP response to CL316243 becomes PTX-sensitive. In contrast, there is no change in the PTX sensitivity of the β_{3b}-AR response. This suggests that residues present in the β_{3a}-AR C-terminal tail may direct localization of the receptor to membrane rafts, and this in turn may govern its capacity to couple to $G\alpha_{i/o}$ proteins. The β_{3a}-AR C terminus, SP^{384}PLNRF^{389}DGY^{392}EGARPF^{398}PT, contains a motif that is similar to the caveolin interaction motif of many proteins ($\phi X\phi XXXX\phi$ or $\phi XXXX\phi XX\phi$, where ϕ is an aromatic residue (23)). We show that cAMP accumulation is PTX-sensitive in cells expressing β_{3a}-ARs carrying mutations in the putative caveolin-binding site. Knockdown of caveolin-1 in CHO-K1 cells expressing the wild type β_{3a}-AR or in mouse brown adipocytes expressing endogenous β_{3a}-ARs also alters the PTX sensitivity of cAMP accumulation and glucose uptake. We demonstrate that caveolin-1 interacts with the wild type β_{3a}-AR but not with mutant β_{3a}-ARs lacking key residues within the interaction motif. Our findings also indicate that PTX treatment increases cAMP responses in membranes derived from cells expressing the β_{3b}-AR via inhibition of receptor-$G\alpha_o$ coupling.

EXPERIMENTAL PROCEDURES

Expression of the Mouse β_{3a}- and β_{3b}-AR and Receptor Mutants in CHO-K1 Cells—Plasmids (pcDNA3.1+) carrying the coding region for each of the β_{3a}- and β_{3b}-AR, a truncated β_3-AR, and the mutant Y392A were as described previously (21, 22). Five additional mutants were created to examine the potential importance of residues in the C terminus for G protein coupling. A construct for expression of the F389A,Y392A,F398A mutant was made by replacing a 561-bp XhoI/XbaI fragment from the wild type β_{3a}-AR plasmid with a PCR fragment generated using the primers mb3.TF, 5′-CGTCTATGCTCGAGTGTTCGTTGTGG-3′ and mb3.FYF-AAA, 5′-CGGTTCTAGACCCTTCACGTGGGA**GC**CGGACGCGCACCTTCA**GC**GCCATCA**GC**CCTGTTGAGC-3′ (restriction sites are underlined and mutated nucleotides are bold). The same strategy was used for the other four mutants, using mb3.TF as the forward primer and the reverse primers mb3.F389A, 5′-CGGTTCTAGACCCTTCACGTGGGAAACGGACGCGCACCTTCATAGCCATCA**GC**CCTGTTGAGC-3′; mb3.F389A/Y392A, 5′-CGGTTCTAGACCCTTCACGTGGGAAACGGACGCGCACCTTCA**GC**GCCATCA**GC**CCTGTTGAGC-3′; mb3.A395E, 5′-CGGTTCTAGACCCTTCACGTGGGAAACGGACGC**T**CACCTTCATAGCCATC-3′; mb3.P384S, 5′-CGGTTCTAGACCCTTCACGTGGGAAACGGACGCGCACCTTCATAGCCATCAAACCTGTTGAGCGGTG**A**ACTCTGCCTG-3′; and mb3.P384S/F389A, 5′-CGGTTCTAGACCCTTCACGTGGGAAACGGACGCGCACCTTCATAGCCATCA**GC**CCTGTTGAGCGGTG**A**ACTCTGCCTG-3′. All PCRs were carried out as described before (22), using Platinum Pfx High Fidelity DNA polymerase (Invitro-

gen). The complete insert and junctions with pcDNA3.1 were confirmed for each of the β_3-AR constructs by DNA sequencing on both strands (Micromon, Monash University, Victoria, Australia).

Cell Culture of CHO-K1 Cells Expressing Mouse β_3-ARs—Chinese hamster ovary (CHO-KI) cells were grown in 50:50 Dulbecco's modified Eagle's medium (DMEM)/Ham's F-12 medium supplemented with 10% (v/v) fetal bovine serum (FBS), glutamine (2 mM), penicillin (100 units/ml), and streptomycin (100 μg/ml) at 37 °C with 5% CO_2. Clonal cell lines expressing the wild type β_{3a}-AR, β_{3b}-AR, and truncated β_3-AR were described previously (21, 22). The cells were maintained in DMEM/Ham's F-12 (50:50) medium containing 10% FBS and 400 μg/ml G418 under 5% CO_2 at 37 °C. CHO-K1 cells expressing mutant β_{3a}-ARs were generated by transient transfection using Lipofectamine, and cAMP assays or the Duolink *in situ* proximity ligation assay were performed 48 h after transfection.

Cell Culture and Transient Transfection of siRNA-Cav1—For transfection, CHO-K1 cells stably expressing the β_{3a}- or β_{3b}-AR were seeded overnight at 3.5×10^5 cells per well in 6-well plates. siRNA constructs were obtained from Dr. Debbie C. Thurmond (Indiana University School of Medicine, Indianapolis) and consisted of siRNA-directed against canine caveolin-1 (GCCCAACAACAAGGCCATG) or siRNA containing a control sequence (GCGCGCTTTGTAGGATTCG) (24). The caveolin-1 siRNA was chosen as it corresponded to a region that was identical across all available mammalian sequences and had been used successfully to knock down expression in CHO-K1 cells (24). 1.5 μg of the caveolin-1 siRNA or control plasmid was transfected using Lipofectamine™ (Invitrogen). For cAMP accumulation assays, cells were plated into 96-well plates, and PTX was added to half the wells 16 h before experiments. Western blotting and cAMP accumulation assays were performed 48 h after the start of transfection.

Immunoblotting to Detect β_3-ARs—Transfected cells were grown in 12-well plates at 1×10^5 cells per well in DMEM/Ham's F-12 medium containing 0.5% FBS overnight. Cells were lysed directly in each well by the addition of 80 μl of 65 °C SDS sample buffer (62.5 mM Tris-HCl, pH 6.8, 2% SDS, 10% glycerol, 50 mM dithiothreitol, and 0.1% bromophenol blue). Cells were scraped, transferred to an Eppendorf tube on ice, and sonicated for 5 s followed by heating to 95 °C for 5 min. Aliquots of the samples were separated on a 10% polyacrylamide gel and electrotransferred to Hybond-P polyvinylidene difluoride membranes (pore size 0.45 μm; Amersham Biosciences) with a semidry electroblotter. After transfer, the membranes were allowed to soak in Tris-buffered saline for 5 min, followed by quenching of nonspecific binding (1 h at room temperature in 5% nonfat dry milk and 0.1% Tween 20 in Tris-buffered saline). Membranes were incubated overnight at 4 °C with primary antibody, β_3-AR (Santa Cruz Biotechnology) diluted 1:1000, or total-AKT (Cell Signaling Technology) diluted 1:1000. This was detected using a secondary antibody (HRP-linked anti-goat IgG, Cell Signaling) diluted 1:2000 and enhanced chemiluminescence (ECL, Amersham Biosciences).

Confirmation of Caveolin-1 siRNA Efficacy by Immunoblotting—Lysates from siRNA-treated cells were prepared as above, resolved on 10% polyacrylamide gels, and transferred to Bio-Rad PVDF membranes. Blots were blocked using 5% BSA dissolved in PBS plus 0.1% Tween 20 (PBS-T) and then probed with a mixture of 1 μg/ml each of rabbit anti-caveolin-1 (AbCam ab2910) and mouse anti-β-actin (ab8226) in 1% BSA in PBS-T plus 0.02% sodium azide. Following washing, blots were probed with mixtures of 1 μg/ml goat anti-mouse AF647 (Molecular Probes A21236) and goat anti-rabbit AF532 (Molecular Probes A11009) in PBS-T containing 0.02% sodium azide. After washing, blots were imaged on a Typhoon Trio (GE Healthcare) using 532 laser 555/20 emission (caveolin-1) and 633 laser 670/30 emission (β-actin).

Animals and Genotyping—All animal studies were approved by the Monash University Animal Ethics Committee. Animals used for experimentation were anesthetized with 80% CO_2, 20% O_2. 3–4-Week-old FVB mice of either sex were bred at Mouseworks (Monash University). Caveolin-$1^{+/+}$ and Caveolin-$1^{-/-}$ mice of either sex (3–4 weeks old) were obtained from Dr. Robin L Anderson (Peter MacCallum Cancer Centre, Melbourne, Australia) with permission from Dr. T. Kurzchalia (25). These mice had been backcrossed for at least 10 generations on a pure BALB/c background (Dr. R. Anderson). Offspring were the product of $+/- \times +/-$ or $+/- \times -/-$ matings because $-/- \times -/-$ matings were not effective. Genomic DNA analysis was conducted on mouse tails to determine the genotype of all mice used for experimental studies before animals were obtained. Genomic DNA was isolated by proteinase K digestion overnight followed by extraction of DNA using a commercial kit (Wizard SV Genomic DNA Purification System, Promega Corp., Alexandria, New South Wales, Australia). PCR was performed on ~20 ng of DNA (50 °C annealing, 35 cycles) using primers designed to indicate the presence/absence of neomycin disruption to the caveolin-1 allele using Go TaqDNA polymerase according to the manufacturer's instructions (Promega). Primers to amplify the caveolin-1 knock-out fragment were forward, 5′-TATTCTGCCTTCCTGATGATAACTG-3′, and reverse, 5′-CCTGCGTGCAATCCATCTTGTTCAATG-3′, and primers to amplify the caveolin-1 wild type fragment were forward, 5′-TTTACCGCTTGTTGTCTACGA-3′, and reverse, 5′-TATCTCTTTCTGCGTGCTGA-3′ (primers from Invitrogen). This generated a wild type product of 240-bp and a knock-out product of 1450 bp. PCR products were run on a 1.3% agarose gel and the bands digitally captured.

Cell Isolation and Culture of Mouse Brown Adipocytes—Brown fat precursor cells were isolated and cultured as described previously (26) with modifications as outlined in Ref. 27. The interscapular, axillary, and cervical brown adipose tissue depots were dissected out under sterile conditions, minced, and transferred to a solution containing 123 mM NaCl, 5 mM KCl, 1.3 mM $CaCl_2$, 5 mM glucose, 1.5% (w/v) crude bovine serum albumin, 100 mM Hepes, pH 7.4, and 0.2% (w/v) crude collagenase type II. Routinely, pooled tissue from two mice was digested in 10 ml of the Hepes-buffered solution. The tissue was digested (30 min, 37 °C) with vortexing every 5 min, and the digest was filtered through a 250-μm filter into sterile tubes. The solution was placed on ice for 15 min to allow the mature

brown fat cells and lipid droplets to float. The infranatant was filtered through a 25-μm filter and collected, and the precursor cells were pelleted by centrifugation (10 min, 700 × *g*), resuspended in Dulbecco's modified Eagle's medium (DMEM) (4.5 g glucose/liter), and re-centrifuged. The pellet was resuspended in 12 ml of DMEM, and the cells were seeded into 24-well plates and grown in DMEM supplemented with 10% (v/v) newborn calf serum, 2.4 nM insulin, 10 mM Hepes, 50 IU/ml penicillin, 50 μg/ml streptomycin, and 25 μg/ml sodium ascorbate. Brown adipocytes were used for experiments following 7 days in culture.

Radioligand Binding Assay—Cell membranes were prepared, and saturation-binding experiments were performed as described previously (21). Briefly, the homogenate (~10–20 μg of protein) was incubated with [^{125}I]iodo-(−)-cyanopindolol (100–2000 pM) for 60 min at room temperature in the absence or presence of (−)-alprenolol (1 mM) to define nonspecific binding. Reactions were terminated by rapid filtration through GF/C filters presoaked for 30 min in 0.5% (v/v) polyethyleneimine using a Packard Cell Harvester, and radioactivity was measured using a Packard Top Count.

cAMP Accumulation Studies—CHO-K1 cells (1×10^4 cells per well) expressing β_3-ARs were grown in 96-well plates in DMEM/Ham's F-12 medium containing 0.5% (v/v) FBS for 2 days. In studies where brown adipocytes were used, all experiments were performed on day 7 of cell culture. On day 6, the cells were serum-starved overnight in DMEM/Nutrient Mix F-12 (1:1) with 4 mM L-glutamine, 0.5% BSA, 2.4 nM insulin, 10 mM Hepes, 50 IU/ml penicillin, 50 μg/ml streptomycin, and 50 μg/ml sodium ascorbate.

On the day of experiment, media were aspirated, and appropriate drugs diluted in stimulation buffer (1 mg/ml BSA, 0.5 mM IBMX, 0.5 M Hepes, pH 7.4, in Hanks' balanced salt solution) were added. After 30 min of incubation at 37 °C, media were removed, and 100 μl of lysis buffer (1 mg/ml BSA, 0.3% (v/v) Tween 20, 0.5 M Hepes, 0.5 mM IBMX, pH 7.4) were added. Samples were rapidly frozen at −70 °C to lyse cells prior to measurement of cAMP. To examine the effect of PTX, cells were treated with PTX (100 ng/ml) for 16 h before stimulation with appropriate drugs. The effects of filipin III were examined by addition of 1 μg/ml filipin III for 1 h prior to stimulation of cells with CL316243 for 30 min. cAMP accumulation was measured utilizing the cAMP αScreen kit (PerkinElmer Life Sciences) as detailed previously (22). All results are expressed as the percentage of the forskolin response (100 μM) in a given experiment.

Glucose Uptake Measurements—Glucose uptake studies were performed as described previously (28, 29). All experiments were performed on day 7 of brown adipocyte culture. On day 6, the cells were serum-starved overnight in DMEM/Nutrient Mix F-12 (1:1) with 4 mM L-glutamine, 0.5% BSA, 2.4 nM insulin, 10 mM Hepes, 50 IU/ml penicillin, 50 μg/ml streptomycin, and 50 μg/ml sodium ascorbate, plus or minus PTX (100 ng/ml). On the morning of day 7, the medium was changed to DMEM without insulin (containing 0.5% BSA, 50 μg/ml of sodium ascorbate) for at least 30 min. Drugs were added and the samples incubated for 110 min in a final volume of 500 μl, and then the medium was discarded, and cells washed with pre-warmed PBS (10 mM phosphate buffer, 2.7 mM KCl, 137 mM NaCl, pH 7.4). Glucose-free DMEM (containing 0.5% BSA, 50 μg/ml sodium ascorbate) was added, and the drug concentrations were re-added with 50 nM 2-deoxy-D-[1-^{3}H]glucose (Amersham Biosciences, specific activity 9.5–12 Ci/mmol) in a total volume of 500 μl for 10 min. Reactions were terminated by rapid aspiration and washing cells twice in ice-cold PBS. Cells were lysed (500 μl of 0.2 M NaOH, 1 h at 55 °C), and the incorporated radioactivity was determined by liquid scintillation counting (the contents of the entire well were transferred to a single scintillation vial). All results are expressed as the percentage of the basal response (defined as 100%) in a given experiment.

cAMP Accumulation and GTPγ^{35}S Binding in Crude Membranes—CHO-K1 cells stably expressing the mouse β_{3a}- or β_{3b}-AR and primary cultures of mouse brown adipocytes were grown to confluence prior to the preparation of crude membranes. Growth media were removed, and cells were washed once in room temperature PBS. Cells were removed with a cell scraper in ice-cold buffer A (20 mM Tris, pH 7.5, 2 mM EDTA, 0.4 mM PMSF, protease inhibitor mixture) and lysed using a 22-gauge needle. The cell suspension was centrifuged (39,000 × *g*, 20 min, 4 °C) before re-homogenization in ice-cold buffer B (50 mM Tris, pH 7.5, 1 mM EDTA, protease inhibitor mixture) using a 25-gauge needle. Protein concentration was measured using a BCA protein assay (Pierce) prior to snap freezing and storage of the crude membranes at −80 °C.

cAMP generated by the crude membranes was measured using an AlphaScreen cAMP accumulation kit according to the manufacturer's instructions (PerkinElmer Life Sciences). Crude membranes were diluted to 1 μg of protein per well in a white 384-well plate in stimulation buffer (50 mM Tris, pH 7.4, 150 mM NaCl, 10 mM $MgCl_2$, 1.5 mM $CaCl_2$, 100 μM ATP, 1 μM GDP, and 1 nM GTP), mixed with anti-cAMP acceptor beads, and incubated for 30 min at room temperature in the dark. Membranes were stimulated with vehicle or CL316243 for 30 min at room temperature in the dark, before the addition of streptavidin-donor beads and biotinylated cAMP diluted in detection buffer (5 mM Hepes, pH 7.4, 0.1% BSA, 0.3% Tween 20). Samples were incubated for 4 h in the dark at room temperature prior to reading the plates on a Fusion-α microplate reader. Data were analyzed against a cAMP standard curve and are expressed as the amount of cAMP generated per μg of crude membrane protein. To examine the effect of pertussis toxin, crude membranes were incubated with 20 μg/ml activated pertussis toxin (5 mM ATP, 5 mM DTT, 30 min at 30 °C, as per manufacturer's instructions) (30, 31) for 15 min at room temperature.

[^{35}S]GTPγS immunoprecipitation was performed to assess direct activation of $G\alpha_s$, $G\alpha_{i1}$, $G\alpha_{i2}$, $G\alpha_{i3}$, or $G\alpha_o$ following stimulation of the mouse β_{3a}- or β_{3b}-adrenergic receptors (32, 33). Reaction tubes were maintained at 30 °C and contained crude membranes (75 μg per reaction) diluted in assay buffer (10 mM Hepes, 100 mM NaCl, 10 mM $MgCl_2$, 1% BSA, 0.01% saponin, pH 7.4). Crude membranes were preincubated for 5 min with 1 μM ($G\alpha_s$ immunoprecipitations) or 10 μM ($G\alpha_{i1}$, $G\alpha_{i2}$, $G\alpha_{i3}$, and $G\alpha_o$ immunoprecipitations) GDP at 30 °C, prior to addition of vehicle or 3 μM CL316243 and 1 nM

[^{35}S]GTPγS (PerkinElmer Life Sciences) for 20 min at 30 °C. The final reaction volume was 100 μl. Reactions were terminated by placing the tubes on ice, and membranes were completely solubilized by the addition of 100 μl of ice-cold solubilization buffer (100 mM Tris, 200 mM NaCl, 1 mM EDTA, 1.25% Nonidet P-40, 0.1% SDS, pH 7.5). Samples were precleared for 90 min at 4 °C by the addition of 10 μl of 10% (v/v) preimmune serum (normal rabbit IgG for $G\alpha_s$ and $G\alpha_{i3}$ immunoprecipitations; normal mouse IgG for $G\alpha_{i1}$, $G\alpha_{i2}$, and $G\alpha_o$ immunoprecipitations, diluted in assay buffer) and 30 μl of 20% (v/v) protein G-agarose (Pierce) that had been diluted in solubilization buffer containing 2% BSA and 0.1% NaN_3. The precleared supernatant (200 μl) was combined with 5 μl of the appropriate $G\alpha$ antibody (1:40 dilution) and rotated at 4 °C overnight. 70 μl of 20% protein G-agarose (as described above) was added, and samples were rotated at 4 °C for 90 min. Beads were washed three times by adding 1 ml of ice-cold solubilization buffer (without SDS), inverting the tubes, and then centrifuging at 500 × *g* for 30 s at 4 °C. After the final wash, the beads were resuspended in 100 μl of solubilization buffer, and scintillation mixture was added, and samples were counted using a liquid scintillation counter.

Duolink^{TM} in Situ Proximity Ligation Assay—The assay was carried out according to the manufacturer's protocol (Olink Biosciences). 24 h after transfection, CHO-K1 cells (1×10^4 cells per well) expressing β_{3a}-ARs as well as the F389, Y392,F398A β_{3a}-AR and P384S,F389A β_{3a}-AR were plated in polystyrene vessel tissue culture-treated glass slides (Falcon^{TM}) in DMEM/Ham's F-12 medium containing 0.5% (v/v) FBS and incubated at 37 °C for 24 h. On the day of the experiment, media were aspirated, and cells were fixed with 4% paraformaldehyde in PBS for 20 min. Cells were washed with PBS and quenched in 50 mM glycine for 5 min. After washing with PBS, cells were permeabilized with 0.25% Triton X-100 for 15 min. Cells were washed with PBS and then blocked in Duolink blocking solution overnight at 4 °C. After cells were washed with PBS, primary antibodies, anti-caveolin-1 (rabbit, 1:1000 dilution, Cell Signaling), and anti-β_3-AR antibody (goat, 1:1000 dilution, Santa Cruz Biotechnology) were added and incubated overnight at 4 °C. Cells were washed with PBS and then secondary antibodies conjugated with oligonucleotides (PLA probe anti-rabbit MINUS and anti-goat PLUS) were added and incubated for 2 h at 37 °C. Cells were washed with PBS and then incubated with Hybridization solution, consisting of two oligonucleotides, for 15 min at 37 °C. After washing with TBS-T, the Ligation solution was added together with ligase for 30 min at 37 °C. Cells were washed with TBS-T, and the Amplification solution, consisting of nucleotides, was added together with polymerase for 90 min at 37 °C. The cells were washed with TBS-T, and the Detection solution, consisting of fluorescently labeled oligonucleotides plus Hoechst 33342 nuclear stain, was added for 1 h at 37 °C. Slides were washed successively in 2× SSC (0.3 M sodium chloride, 0.03 M sodium citrate) for 2 min, 1× SSC for 2 min, 0.2× SSC for 2 min, 0.02× SSC for 2 min, and 70% EtOH for 1 min and mounted with ProLong Gold antifade reagent (Invitrogen), and a cover glass was placed on the sample. Cells were observed in a Leica DMLB epifluorescence microscope. Photographs were taken at ×63 magnification, and images were acquired by using a DC350F camera and IM500 software (Leica Microsystems AB; Kista, Sweden).

Data Analysis—All results are expressed as a means ± S.E. of *n*. Data were analyzed using nonlinear curve fitting (GraphPad PRISM version 5.0) to obtain pEC_{50} values where appropriate or using a one-site fit to obtain K_D and B_{max} values (saturation binding experiments). Statistical significance was determined using two-way ANOVA tests or Student's *t* test. Probability values less than or equal to 0.05 were considered significant.

Drugs and Reagents—Drugs and reagents were purchased as follows: 2-deoxy-D-[1-^{3}H]glucose (specific activity 9.5–12 Ci/mmol) (Amersham Biosciences); G418 (Calbiochem); HRP-linked anti-rabbit IgG, Akt antibody, caveolin-1 antibody (Cell Signaling Technology, Beverly, MA); anti-β_3-AR antibody, anti-$G\alpha_s$, $G\alpha_{i1}$, $G\alpha_{i2}$, $G\alpha_{i3}$, and $G\alpha_o$ antibodies (Santa Cruz Biotechnology); normal rabbit/mouse IgG, protein-G agarose (Pierce); Duolink^{TM} *in situ* proximity ligation assay kit (Olink Bioscience, Uppsala, Sweden); [^{125}I]iodo-(−)-cyanopindolol (2200 Ci/mmol, ProSearch International Australia Pty Ltd., Melbourne, Australia); aprotinin, leupeptin, and pepstatin A (ICN, Costa Mesa, CA); Lipofectamine, OptiMEM® (Invitrogen); insulin (Actrapid®) (Novo Nordisk, Bagsvaerd, Denmark); cAMP α-screen kit, GTPγ^{35}S (PerkinElmer Life Sciences); (−)-alprenolol, bacitracin, CL316243 ((*R*,*R*)-5-[2-[[2-(3-chlorophenyl)-2-hydroxyethyl]-amino]-propyl]1,3-benzodioxole-2,2-decarboxylate), filipin III, IBMX, pertussis toxin, polyethyleneimine, (Sigma). All cell culture media and supplements were obtained from Trace Biosciences (Castle Hill, New South Wales, Australia). All other drugs and reagents were of analytical grade.

RESULTS

Differential PTX Sensitivity of cAMP Accumulation Mediated by β_3-AR Isoforms—The two β_3-AR isoforms share a common proximal C-terminal region but differ at the distal C terminus (Fig. 1*A*). We examined the properties of the wild type β_{3a}-AR, β_{3b}-AR, and a truncated β_3-AR that lack the C-terminal tail of either splice variant in clonal CHO-K1 cell lines with equivalent receptor densities (B_{max} 1148 ± 241, 1309 ± 128, and 1224 ± 105 fmol/mg protein, respectively). Maximal cAMP responses to the selective β_3-AR agonist CL316243 in cells expressing the β_{3a}-AR were unaffected by pretreatment of cells with PTX (100 ng/ml, 16 h; Fig. 1*B* and supplemental Table S1), whereas responses in cells expressing the β_{3b}-AR increased by 36% following pretreatment with PTX ($p < 0.0001$; Fig. 1*C*), confirming our previous results (22). The pEC_{50} values for CL316243 at β_{3a}- and β_{3b}-AR were not significantly different and were not altered significantly by PTX pretreatment (supplemental Table S1). The truncated β_3-AR behaved similarly to the β_{3b}-AR and displayed PTX sensitivity (Fig. 1*D* and supplemental Table S1). This suggested that rather than the β_{3b}-AR containing a motif that enables coupling to $G\alpha_{i/o}$, the C terminus of the β_{3a}-AR contains a motif that disables coupling to the inhibitory G protein. Our previous study indicated that this β_{3a}-AR motif interferes with $G\alpha_{i/o}$ coupling by effects on receptor localization and/or protein-protein interactions (22). In essence, the PTX resistance of β_{3a}-AR responses provides a

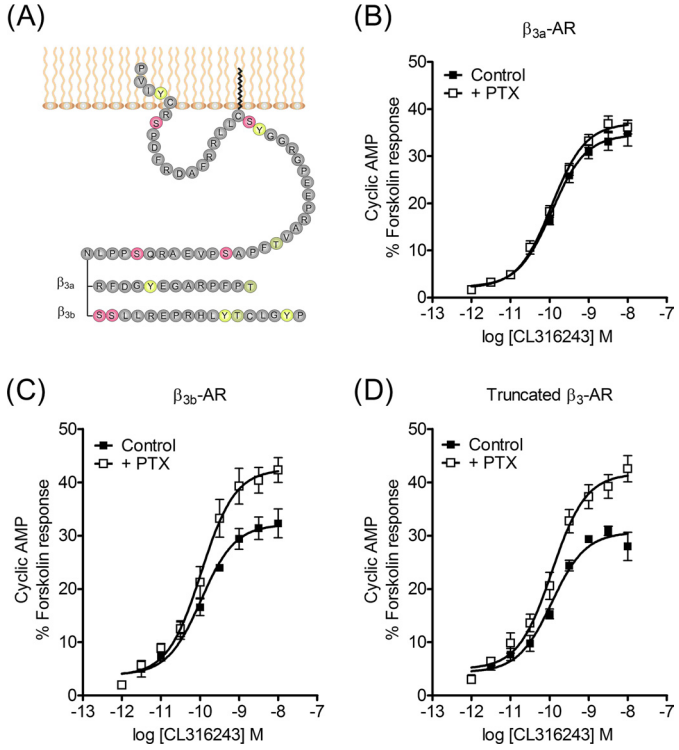

FIGURE 1. **Functional responses following activation of β_3-AR isoforms.** *A*, snake diagram of the C-terminal tail of β_3-AR isoforms. Note that the truncated mutant terminates at residue Asn-387. *B–D,* concentration-response curves for stimulation of cAMP accumulation by the β_{3a}-AR (*B*), β_{3b}-AR (*C*), and truncated β_3-AR (*D*) in the presence or absence of pretreatment with PTX (100 ng/ml, 16 h). CHO-K1 cells stably expressing each β_3-AR were exposed to CL316243 for 30 min in stimulation buffer containing 0.5 mM IBMX to inhibit phosphodiesterases. Responses to forskolin (10^{-4} M) were determined in parallel with agonist-stimulated cAMP accumulation for each batch of cells, and results are expressed as a % of the response to forskolin. Basal cAMP and responses to 100 μM forskolin (*fsk*) were in control basal 0.33 ± 0.13 and fsk 17.2 ± 4.2 pmol/10^4 cells; +PTX basal 0.33 ± 0.13 and fsk 18.1 ± 5.5 pmol/10^4 cells (*B*); control basal 0.27 ± 0.16 and fsk 22.4 ± 4.2 pmol/10^4 cells; +PTX basal 0.41 ± 0.12 and fsk 21.8 ± 2.7 pmol/10^4 cells (*C*); control basal 0.78 ± 0.21 and fsk 22.5 ± 4.1 pmol/10^4 cells; +PTX basal 0.68 ± 0.17 and fsk 23.1 ± 3.3 pmol/10^4 cells (*D*). cAMP accumulation responses were PTX-sensitive in cells expressing the β_{3b}-AR and truncated receptor ($p < 0.001$ determined by two-way ANOVA) but not the β_{3a}-AR. Values are means ± S.E. of 4–5 independent experiments.

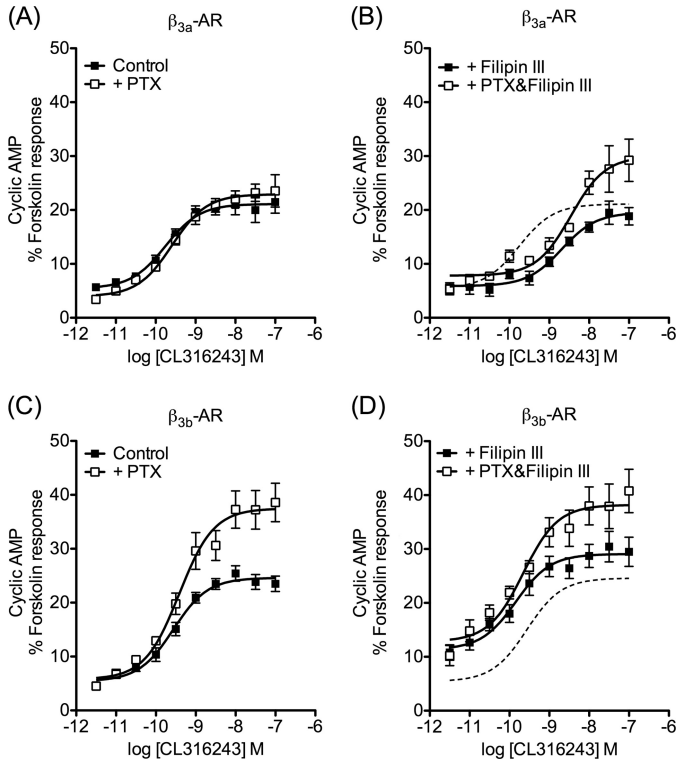

FIGURE 2. **Disruption of caveolae by filipin III alters functional responses of β_3-AR isoforms.** Concentration-response curves were constructed for stimulation of cAMP accumulation by CL316243 in the presence or absence of filipin III (1 μg/ml, 1 h) or following pretreatment of cells with PTX (100 ng/ml, 16 h). In cells stably expressing the β_{3a}-AR, cAMP accumulation was not altered by PTX treatment (*A*), but the addition of filipin III caused the response to become PTX-sensitive (*B*, $p < 0.001$ determined by two-way ANOVA). In cells expressing the β_{3b}-AR isoform, filipin III did not have a significant effect on PTX-sensitivity (*C* and *D*). Basal cAMP and responses to 100 μM fsk were in control basal 1.23 ± 0.47 and fsk 24.4 ± 9.7 pmol/10^4 cells; +PTX basal 0.85 ± 0.36 and fsk 24.6 ± 10.4 pmol/10^4 cells (*A*); control basal 1.45 ± 0.64 and fsk 23.0 ± 9.5 pmol/10^4 cells; +PTX basal 1.35 ± 0.62 and fsk 22.5 ± 10.6 pmol/10^4 cells (*B*); control basal 1.06 ± 0.40 and fsk 23.1 ± 8.3 pmol/10^4 cells; +PTX basal 1.35 ± 0.55 and fsk 27.1 ± 9.3 pmol/10^4 cells (*C*); control basal 2.56 ± 0.88 and fsk 27.0 ± 9.6 pmol/10^4 cells; +PTX basal 2.29 ± 0.80 and fsk 26.1 ± 9.5 pmol/10^4 cells (*D*). *B* and *D*, *dotted* line shows the concentration-response curve for CL316243 in the absence of filipin III or PTX pretreatment, taken from *A* or *C*, respectively, for comparison. In CHO-β_{3a}-AR cells filipin III caused a right shift of the curve, whereas in CHO-β_{3b}-AR cells, basal and maximal cAMP accumulation were increased, but there was no change in the potency of CL316243. Results are expressed as a % of the response to forskolin (10^{-4} M), and values are means ± S.E. of 4–6 independent experiments.

functional readout of the capacity of the C terminus to direct this localization or interaction.

Signaling by β_3-AR Isoforms Is Differentially Affected by Filipin Treatment—As the behavior of the β_2-AR and other GPCRs are affected by localization in membrane raft domains (12), we examined the effect of disrupting membrane rafts using filipin III. In cells expressing the β_{3a}-AR, PTX pretreatment had no effect on cAMP accumulation in response to CL316243 as described previously (21, 22). However, after treatment with filipin III (1 μg/ml), the cAMP response to CL316243 became PTX-sensitive, with the maximum response being increased by 55% (supplemental Table S1 and Fig. 2*B*). Interestingly, the concentration-response curve was also markedly shifted to the right in the presence of filipin III (pEC_{50} control 9.76 ± 0.14, + filipin III 8.69 ± 0.15, $p < 0.01$), and an equivalent negative effect of filipin III on the potency of CL316243 was seen in the presence of PTX (supplemental Table S1).

In cells expressing the β_{3b}-AR, pretreatment with PTX caused a 36% increase in the maximum cAMP response to CL316243, with no change in the pEC_{50} value (Fig. 2*C*). Filipin III treatment (1 μg/ml) significantly increased the basal level of cAMP; however, PTX pretreatment followed by filipin III still caused an increase in the maximum response to CL316243 by 38% compared with cells treated with filipin III alone (Fig. 2*D* and supplemental Table S1). Filipin III had no significant effect on the pEC_{50} of CL316243 relative to control cells, indicating that the rightward shift in β_{3a}-AR-expressing cells was not an artifact associated with overall effects on cell signaling or viability. Thus, treatment with filipin III facilitated coupling of the β_{3a}-AR isoform to $G\alpha_{i/o}$ and possibly reduced efficiency of coupling to the cAMP pathway, but it had no effect on agonist-stimulated β_{3b}-AR responses.

Note that the E_{max} and pEC_{50} values for the filipin experiment are lower than those seen in Fig. 1 for both the β_{3a}- and β_{3b}-AR expressing cells. We are making comparisons only

within a given experiment, however, where cells at equivalent confluence and passage number were treated in parallel with PTX/vehicle and then with filipin III/vehicle.

Effect of siRNA Knockdown of Caveolin-1 on cAMP Signaling Mediated by the β_3-AR—Treatment of cells with filipin III disrupts membrane rafts globally, so we next used a more targeted approach by reducing caveolin-1 expression. CHO-K1 cells stably expressing either the β_{3a}- or the β_{3b}-AR were transiently transfected with siRNA directed against caveolin-1 or an siRNA comprising a scrambled form of the same sequence (24). After 48 h of incubation, cells were used for cAMP accumulation assays and analyzed for abundance of caveolin-1 protein. Transfection of cells expressing either the β_{3a}- or the β_{3b}-AR with the siRNA directed against caveolin-1 but not the control sequence caused knockdown of caveolin-1 expression as shown in Fig. 3*A*. Caveolin-1 siRNA treatment of β_{3a}-AR-expressing cells caused the cAMP responses to become PTX-sensitive (Fig. 3*B*), whereas cAMP responses in cells expressing β_{3a}-AR and treated with the negative control sequence were unaltered (Fig. 3*C*). In contrast, transfection of cells expressing the β_{3b}-AR with either the caveolin-1 scrambled sequence or caveolin-1 siRNA did not affect the PTX sensitivity of cAMP responses (Fig. 3, *D* and *E*). Treatment of cells expressing the β_{3a}-AR with filipin III caused a 10-fold reduction in the potency of CL316243 (Fig. 2*B* and supplemental Table S1), whereas knockdown of caveolin-1 had no effect on potency in the presence or absence of PTX (Fig. 3, *B* and *D*, and supplemental Table S1). Thus filipin III and knockdown of caveolin-1 both promote PTX sensitivity of β_{3a}-AR responses, but filipin III has additional effects on the efficiency of signaling to the cAMP pathway.

Mutations of a Putative Caveolin-binding Site in the C Terminus of the β_{3a}-AR Alter Signaling Properties—The capacity of caveolin-1 siRNA to alter the signaling properties of the β_{3a}-AR indicated that there were amino acid residues or a motif unique to the β_{3a}-AR C terminus that confers interaction with caveolin-1. The β_{3a}-AR C terminus includes the sequence R$\underline{F}^{389}$DG$\underline{Y}^{392}$EGARP$\underline{F}^{398}$PT (Fig. 4*A*), which has three aromatic residues and resembles the caveolin interaction motif of many proteins (23). We previously showed that mutation of Tyr-392 to Ala does not affect β_{3a}-AR cAMP responses, whereas removal of the unique C terminus causes cAMP responses to become PTX-sensitive (22). In this study we have extended this observation by comparing the β_{3a}-, β_{3b}-, and truncated β_3-AR with new mutant receptors lacking single or multiple residues implicated in caveolin-1 binding. As seen with the Y392A β_{3a}-AR, PTX sensitivity was not conferred by the single mutation F389A (supplemental Table S2) or by mutation of the four C-terminal residues (P$\underline{F}$PT) to alanine (data not shown). In cells expressing β_{3a}-ARs mutated at either two or three of the aromatic residues, namely F389A,Y392A, or F389A,Y392A,F398A, CL316243-stimulated cAMP accumulation was increased by 39 or 46%, respectively, in the presence of PTX (Fig. 4, *E* and *F*). Although this indicates that the aromatic residues participate in an interaction that prevents $G\alpha_{i/o}$ coupling, this finding did not appear at first sight to be consistent with a previous demonstration that the rat β_3-AR expressed in the same cell background does couple to $G\alpha_{i/o}$ (34). The rat

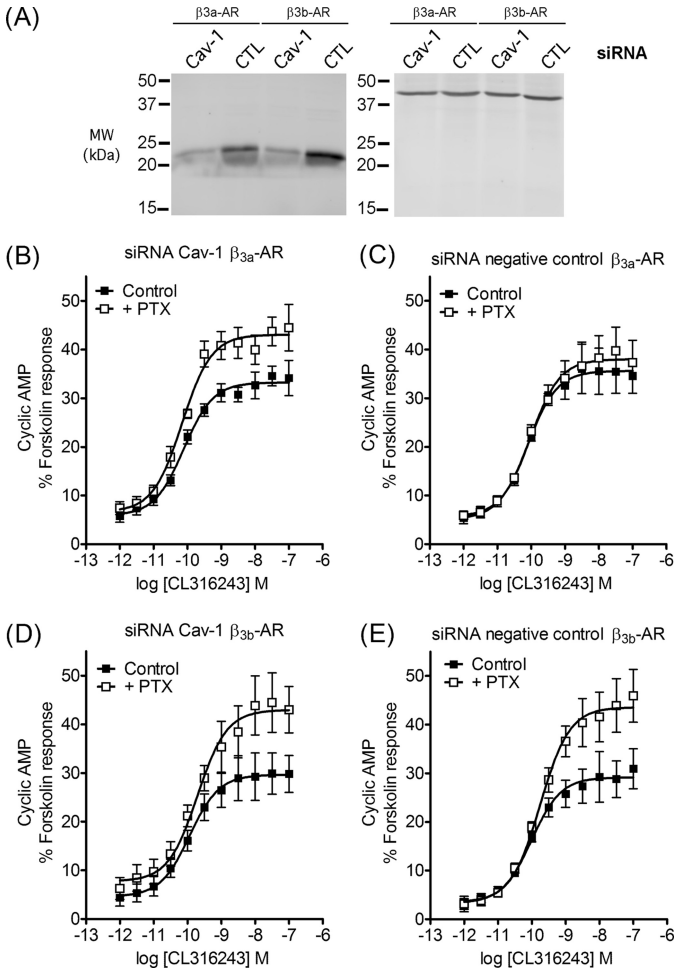

FIGURE 3. **Knockdown of caveolin-1 by siRNA influences responses mediated by β_{3a}- but not β_{3b}-AR.** *A,* siRNA constructs were tested by immunoblotting protein extracts using a caveolin-1 antibody (*left panel*) or β-actin antibody (*right panel*). Equal volumes of cell lysate were subjected to 10% SDS-PAGE prior to immunoblotting. Approximate molecular masses are indicated on the *left* in kDa. A typical immunoblot from four experiments is shown. The *left panel* shows that the caveolin-1 siRNA produced substantial knockdown of caveolin-1 compared with the control siRNA in cells expressing either the β_{3a}-AR or β_{3b}-AR. *B–E*, concentration-response curves were constructed for stimulation of cAMP accumulation by CL316243 in CHO-K1 cells stably expressing β_{3a}- or β_{3b}-AR and transiently transfected with a negative control (*CTL*) or caveolin-1 (*Cav-1*) siRNA construct. Basal cAMP and responses to 100 μM fsk were in control basal 1.47 ± 0.33 and fsk 27.9 ± 3.7 pmol/10^4 cells; +PTX basal 1.49 ± 0.24 and fsk 25.4 ± 5.6 pmol/10^4 cells (*B*); control basal 0.97 ± 0.19 and fsk 22.0 ± 3.5 pmol/10^4 cells; +PTX basal 1.22 ± 0.09 and fsk 24.2 ± 2.9 pmol/10^4 cells (*C*); control basal 1.08 ± 0.47 and fsk 21.7 ± 2.0 pmol/10^4 cells; +PTX basal 1.75 ± 0.73 and fsk 23.0 ± 2.3 pmol/10^4 cells (*D*); control basal 0.76 ± 0.23 and fsk 26.7 ± 4.1 pmol/10^4 cells; +PTX basal 0.65 ± 0.29 and fsk 22.6 ± 4.8 pmol/10^4 cells (*E*). In CHO-β_{3a}-AR cells, knockdown of caveolin-1 caused cAMP accumulation to become PTX-sensitive (*B*, $p < 0.001$ determined by two-way ANOVA), whereas the negative control siRNA had no effect (*C*). In CHO-β_{3b}-AR cells, neither the caveolin-1 siRNA nor the negative control siRNA had any effect on PTX sensitivity (*D* and *E*). Results are expressed as a % of the response to forskolin (10^{-4} M), and values are means ± S.E. of six independent experiments.

β_3-AR C terminus (R$\underline{F}^{389}$DG$\underline{Y}$392EG$\underline{E}$RP$\underline{F}$398PT) only differs from the mouse β_{3a}-AR sequence at position 395, where it has a glutamate residue instead of alanine. However, when we made a mutant A395E mouse β_{3a}-AR, cAMP accumulation was still PTX-resistant (Fig. 4*C* and supplemental Table S2). We therefore tested the idea that there must be additional residues outside the unique β_{3a}-AR tail that influence $G\alpha_{i/o}$ coupling. One

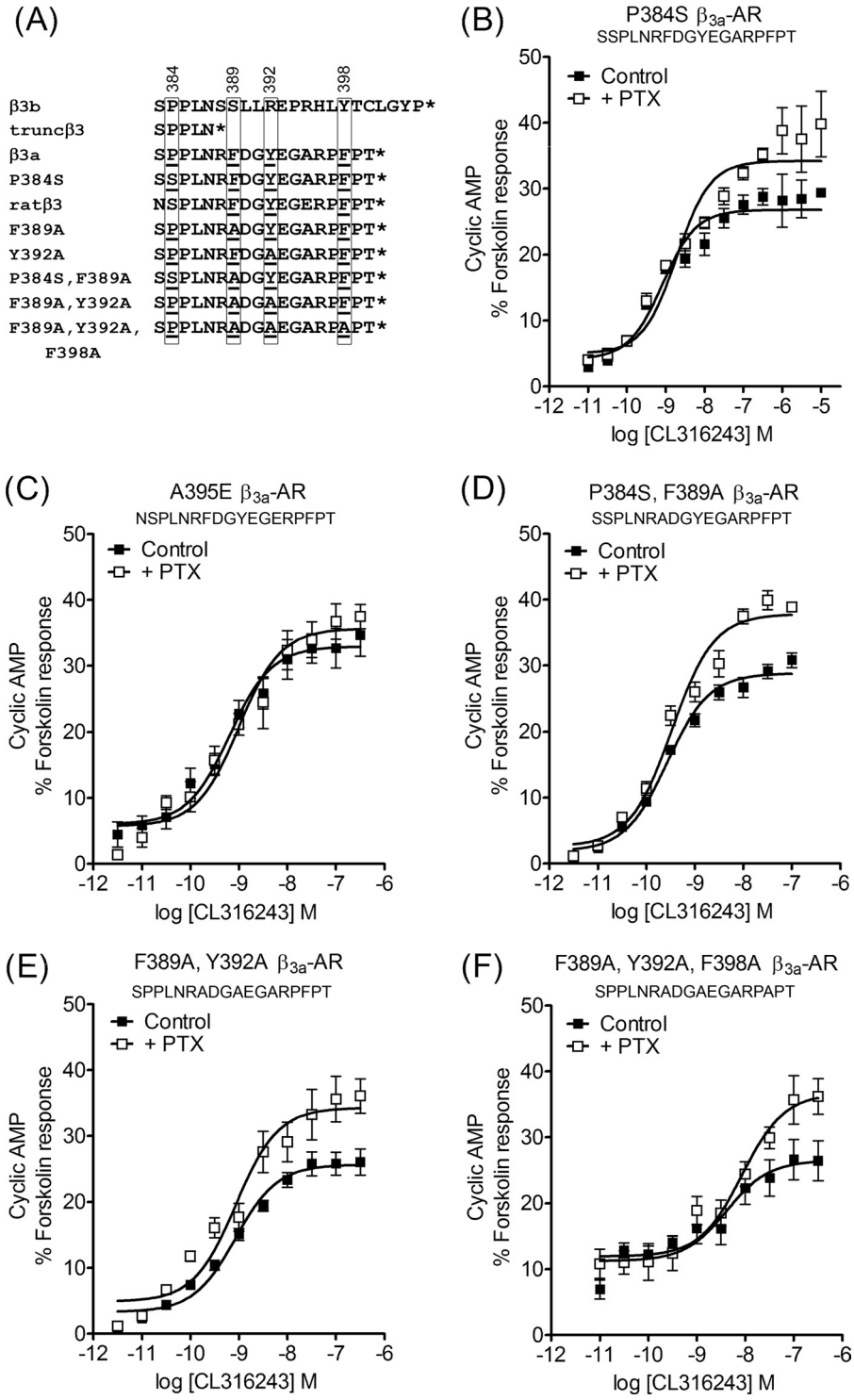

FIGURE 4. **Site-directed mutagenesis of putative sites in the β_{3a}-AR C terminus involved in interactions with caveolin-1.** The C-terminal sequences of all relevant mouse β_3-AR isoforms and mutants, plus the rat β_3-AR, are shown in *A*. The residue at position 384 and aromatic residues at positions 389, 392, and 398 are *boxed*. Concentration-response curves were constructed for stimulation of cAMP accumulation by CL316243 in CHO-K1 cells transiently transfected with mutant β_{3a}-ARs. Pretreatment with PTX (100 ng/ml, 16 h) increased maximal cAMP accumulation in cells expressing the P384S β_{3a}-AR (*B*), P384S,F389A β_{3a}-AR (*D*), F389A,Y392A β_{3a}-AR (*E*), or F389A,Y392A,F398A β_{3a}-AR (*F*) mutants ($p < 0.001$ determined by two-way ANOVA), but not the A395E β_3-AR (*C*). Basal cAMP and responses to 100 μM fsk were as follows: *B*, control basal 0.13 ± 0.03 and fsk 9.3 ± 2.3 pmol/10^4 cells; +PTX basal 0.16 ± 0.06 and fsk 9.9 ± 2.5 pmol/10^4 cells; *C*, control basal 0.58 ± 0.25 and fsk 8.5 ± 1.1 pmol/10^4 cells; +PTX basal 0.18 ± 0.07 and fsk 8.1 ± 1.3 pmol/10^4 cells; *D*, control basal 0.11 ± 0.02 and fsk 12.6 ± 5.9 pmol/10^4 cells; +PTX basal 0.08 ± 0.01 and fsk 11.5 ± 5.5 pmol/10^4 cells; *E*, control basal 0.17 ± 0.05 and fsk 8.5 ± 0.9 pmol/10^4 cells; +PTX basal 0.19 ± 0.05 and fsk 10.0 ± 1.3 pmol/10^4 cells; *F*, control basal 0.60 ± 0.24 and fsk 9.1 ± 4.3 pmol/10^4 cells; +PTX basal 0.87 ± 0.44 and fsk 10.0 ± 4.3 pmol/10^4 cells. Results are expressed as a % of the response to forskolin (10^{-4} M), and values are means ± S.E. of 4–6 independent experiments. The ^{389}P*XXXX*F^{389}*XX*Y^{392} motif appears to be dominant in modulating $G\alpha_{i/o}$ coupling of the β_3-AR isoforms.

possibility is that the caveolin-1 interaction motif actually starts within a region common to the β_{3a}- and β_{3b}-AR isoforms. Although there are no aromatic residues in the region upstream of Phe-389, there is a hydrophobic proline residue at position 384 in the mouse β_{3a}-AR that creates a motif with the spacing P*XXXX*F*XX*Y (mouse SP^{384}PLNRF^{389}DGY^{392}EGARPFPT; rat NS^{384}PLNRF^{389}DGY^{392}EGERPFPT). Therefore, we made a P384S mutation in the mouse β_{3a}-AR, either alone or in combination with F389A. The P384S,F389A double mutant and even the P384S single mutant receptor displayed 30 and 28% increases in cAMP accumulation following PTX treatment (Fig. 4, *B* and *D*), slightly less than the increases seen with the F389A,Y392A (Fig. 4*E*) and F389A,Y392A,F398A (Fig. 4*F*) mutants (supplemental Table S2). The combined mutation data suggest that the motif P*XXXX*F*XX*Y is the dominant factor in determining $G\alpha_{i/o}$ coupling properties of the mouse β_{3a}-AR (Fig. 4*A*).

It is important to note that all mutation studies were done in transiently transfected CHO-K1 cells. The key comparison in each case was between control and PTX-treated samples derived from the same population of transfected cells, and we can therefore make direct comparisons of maximal responses and pEC_{50} values in the absence or presence of PTX for a given cell population but not between cells transfected with different mutant receptors. Variation in the potency of CL316243 between mutants most likely reflects differences in surface expression of the receptors (supplemental Table S2), as we have seen previously (35). It is clear, however, that there is no consistent correlation between pEC_{50} values and the impact of mutations on PTX sensitivity.

Interaction between β_{3a}-AR and Caveolin-1 Requires an Intact Caveolin-1-binding Site—The functional studies described here indicate that mutation of the putative caveolin-binding site enables the modified β_{3a}-AR to couple to both $G\alpha_s$ and $G\alpha_{i/o}$ and suggest that an interaction between the β_{3a}-AR and caveolin-1 modulates cAMP signaling and disables coupling between the β_{3a}-AR and $G\alpha_{i/o}$. To examine interactions between the β_{3a}-AR and caveolin-1, we used a Duolink *in situ* proximity ligation assay (36). We compared untransfected CHO-K1 cells, cells expressing wild type β_{3a}-AR (cAMP responses not sensitive to PTX), and cells expressing either F389A,Y392A,F398A β_{3a}-AR or the P384S,F389A β_{3a}-AR (both cAMP responses PTX-sensitive but to slightly different degrees). Only cells expressing the β_{3a}-AR produced a robust red fluorescent signal (Fig. 5*B*) suggesting that only receptors possessing an intact caveolin-1-binding motif were able to interact with caveolin. Untransfected CHO-K1 cells (Fig. 5*A*) or cells expressing the F389A,Y392A,F398A β_{3a}-AR (Fig. 5*C*) produced no reaction product with the *in situ* proximity ligation assay. Consistent with a somewhat diminished PTX sensitivity, the P384S,F389A β_{3a}-AR showed very low levels of red fluorescence, suggesting a weak interaction with caveolin-1 (Fig. 5*D*). We confirmed expression of wild type and mutant β_{3a}-ARs in the cells used for this assay by immunoblotting (Fig. 5*E*). Note that this experiment could not be performed with the β_{3b}-AR as the β_3-AR antibody used recognizes the C-terminal tail of wild type and mutant β_{3a}-ARs but not the β_{3b}-AR (Fig. 5*E*).

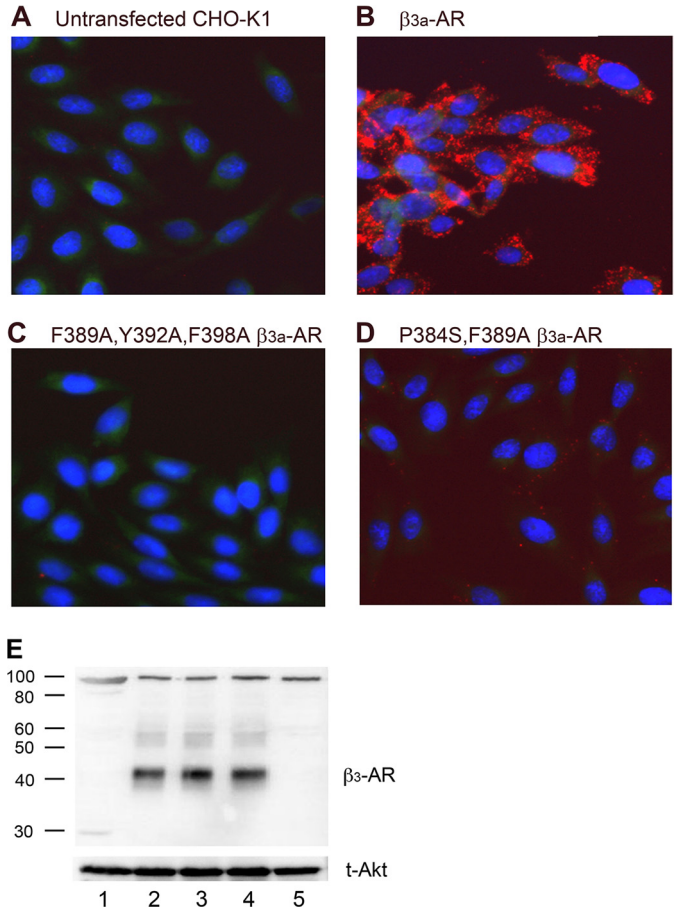

FIGURE 5. **Detection of interactions between β_3-ARs and caveolin-1 using the Duolink™ *in situ* proximity ligation assay.** *A,* untransfected CHO-K1 cells; *B,* CHO-K1 cells expressing the wild type β_{3a}-AR; *C,* F389A,Y392A,F398A β_{3a}-AR; or *D,* P384S,F389A β_{3a}-AR. Cells were fixed on glass slides and incubated with anti-β_3-AR and anti-caveolin-1 primary antibodies and then PLA probe MINUS and PLUS secondary antibodies, as described under "Experimental Procedures." Cells were then treated with hybridization solution containing appropriate oligonucleotides that hybridize to the two PLA probes if they are in close proximity. Hybridized oligonucleotides were ligated and subjected to rolling-circle amplification, and then the concatameric product was detected using fluorescently labeled oligonucleotides. The detection solution also contained Hoechst 33342 nuclear stain. After washing, fluorescence was detected using a Leica DMLB epifluorescence microscope. Photographs were taken at ×63 magnification, and images were acquired using a DC350F camera and IM500 software (Leica Microsystems AB). Cells expressing the wild type β_{3a}-AR displayed robust red fluorescence indicating interaction with caveolin-1 (*B*), whereas nontransfected cells or those expressing the F389A,Y392A,F398A mutant gave no signal (*A* and *C*). There was detectable fluorescence in cells expressing the P384S,F389A β_{3a}-AR, suggesting a weak caveolin-1 interaction (*D*). *E,* expression of each receptor and recognition by the β_3-AR antibody was verified by immunoblotting protein extracts using the β_3-AR antibody (*upper panel*) or t-Akt antibody (*lower panel*). Samples are numbered as follows: *lane 1,* untransfected CHO-K1 cells; *lane 2,* wild type β_{3a}-AR; *lane 3,* F389A,Y392A,F398A β_{3a}-AR; *lane 4,* P384S,F389A β_{3a}-AR; and *lane 5,* β_{3b}-AR. Approximate molecular masses are indicated on the *left* in kDa. Note that the wild type and both mutant β_{3a}-ARs are recognized by the β_3-AR antibody, whereas the β_{3b}-AR does not cross-react with this antibody.

Functional Studies in Brown Adipocytes That Physiologically Express High Levels of β_{3a}-AR—The β_{3a}-AR mRNA transcripts make up >92% of total β_3-AR transcripts in mouse brown adipocytes (20, 37). BAT was therefore chosen as a suitable tissue to test the likely physiological significance of the findings. CL316243 caused a concentration-dependent increase in cAMP levels in primary brown adipocytes from FVB mice, which was unaffected by pretreatment with PTX (Fig. 6*A*).

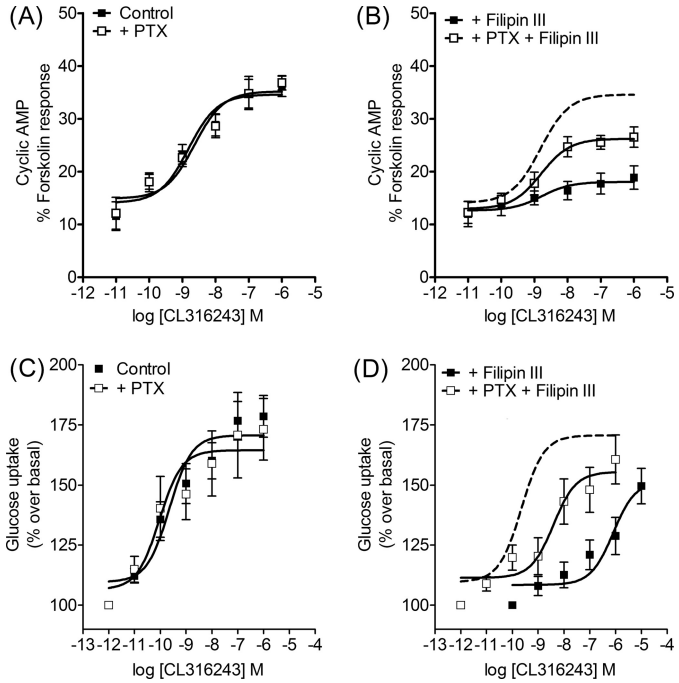

FIGURE 6. **Disruption of caveolae by filipin III alters responses to CL316243 in mouse brown adipocytes that express endogenous β_{3a}-ARs.** Concentration-response curves were constructed for stimulation of cAMP accumulation by CL316243 or glucose uptake in the presence or absence of filipin III (1 μg/ml, 1 h) or following pretreatment of cells with PTX (100 ng/ml, 16 h). In brown adipocytes, cAMP accumulation was not altered by PTX treatment (*A*), but the addition of filipin III (*B*) significantly reduced the maximum response ($p < 0.0001$) but also caused the response to become PTX-sensitive ($p < 0.001$ determined by two-way ANOVA). cAMP accumulation is expressed as a % of the response to forskolin (10^{-4} M), and values are means ± S.E. of seven independent experiments. Basal cAMP and responses to 100 μM fsk were as follows: *A,* control basal 1.3 ± 0.4 and fsk 12.2 ± 1.3 pmol/well; +PTX basal 1.1 ± 0.3 and fsk 12.0 ± 2.7 pmol/well; *B,* filipin III basal 1.2 ± 0.2 and fsk 13.9 ± 2.1 pmol/well; +PTX basal 1.3 ± 0.3 and fsk 14.0 ± 1.7 pmol/well. Examination of a downstream response, glucose uptake, expressed as % over basal, also showed a lack of PTX sensitivity (*C*)., whereas filipin III treatment (*D*) caused a marked shift to the right of the concentration-response curve that was significantly shifted back to the left by PTX pretreatment ($p < 0.001$ determined by two-way ANOVA). Values are means ± S.E. of 8–13 independent experiments. Basal glucose uptake and maximum responses to CL316243 were in control basal 810 ± 64, maximum 1411 ± 118 dpm/well; +PTX basal 760 ± 82, maximum 1332 ± 107 dpm/well (*C*); filipin III basal 1076 ± 121, maximum 1547 ± 164 dpm/well; +PTX basal 883 ± 115, maximum 1475 ± 92 dpm/well (*D*). *B* and *D, dotted line* shows for comparison the concentration-response curve for CL316243 in the absence of filipin III or PTX pretreatment, taken from *A* or *C*, respectively.

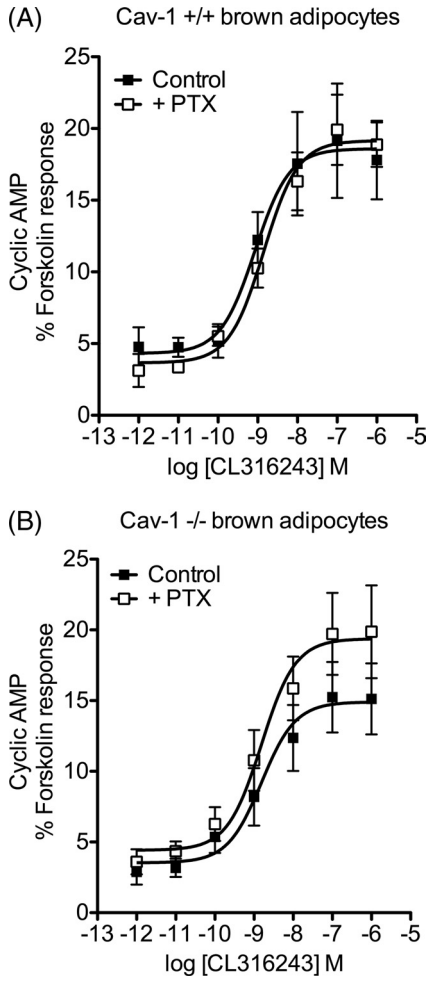

FIGURE 7. **Brown adipocytes isolated from caveolin-1 knock-out mice display altered signaling characteristics.** Concentration-response curves were constructed for stimulation of cAMP accumulation by CL316243 in brown adipocytes cultured from wild type (+/+, *A*) or caveolin-1 knock-out (−/−, *B*) mice. Pretreatment of adipocytes with PTX (100 ng/ml, 16 h) increased CL316243-stimulated cAMP accumulation in adipocytes from the caveolin-$1^{-/-}$ mice ($p < 0.05$ determined by two-way ANOVA) but not in those from wild type mice. Results are expressed as a % of the response to forskolin (10^{-4} M), and values are means ± S.E. of 6–7 independent experiments. Basal cAMP and responses to 100 μM fsk were as follows: *A*, control basal 0.70 ± 0.26 and fsk 16.7 ± 2.0 pmol/well; +PTX basal 0.42 ± 0.25 and fsk 15.8 ± 2.5 pmol/well; *B,* basal 0.45 ± 0.20 and fsk 14.5 ± 3.4 pmol/well; +PTX basal 0.55 ± 0.24 and fsk 14.3 ± 3.2 pmol/well.

Treatment with filipin III (1 μg/ml) significantly reduced the cAMP response to CL316243 ($p < 0.0001$), indicating that disruption of membrane rafts reduced the efficiency of the G_s/AC/cAMP pathway. However, addition of filipin III to cells pretreated with PTX caused a 40% increase in the maximum cAMP response compared with cells treated with filipin III alone ($p < 0.0001$) (Fig. 6*B* and supplemental Table S3). Thus, as in CHO β_{3a}-AR cells, treatment with filipin III caused cAMP responses in BAT to become PTX-sensitive, suggesting enabling of coupling to $G\alpha_{i/o}$.

We also examined a downstream consequence of β_{3a}-AR activation in BAT, namely the facilitation of glucose uptake. CL316243 increased glucose uptake in FVB brown adipocytes as described previously (27, 37), and this response was not significantly affected by PTX pretreatment (Fig. 6*C*). After filipin III treatment (1 μg/ml), the concentration-response relationship for increases in glucose uptake with CL316243 was substantially shifted to the right (Fig. 6*D*). However, in the presence of filipin III and after pretreatment with PTX, the concentration-response curve was shifted back to the left. Thus, in this case, the PTX influence on the sensitivity of the response is manifested as an increase in CL316243 potency rather than as a greater maximum response, perhaps reflecting the difference between an output that is proximal to receptor-Gα coupling *versus* glucose uptake, a downstream signaling event that would display much greater signal amplification.

We also utilized brown adipocytes isolated from WT BALB/c mice and caveolin-1 knock-out (cav-$1^{-/-}$) mice. Whereas brown adipocytes from cav-$1^{+/+}$ mice displayed the normal PTX-insensitive β_{3a}-AR cAMP response, brown adipocytes from cav-$1^{-/-}$ mice displayed cAMP responses that were PTX-sensitive (Fig. 7). Thus, these studies conducted in primary

brown adipocytes isolated from WT and cav-$1^{-/-}$ mice provide supporting evidence that interaction between the β_{3a}-AR and caveolin determines the signaling characteristics of this receptor.

Confirmation That PTX Sensitivity of the β_{3b}-AR Response Is Due to $G\alpha_{i/o}$ Coupling—Our data demonstrate that membrane localization and caveolin interaction influence whether cAMP accumulation is sensitive to pretreatment of cells with PTX. We sought to confirm that the PTX sensitivity of the β_{3b}-AR response does reflect coupling of this isoform to $G\alpha_{i/o}$ proteins, as an alternative explanation is that PTX acts primarily by relieving tonic inhibition of adenylyl cyclase (AC) by $G\alpha_{i/o}$. The β_{3b}-AR may occupy cellular compartments enriched for AC and/or $G\alpha_{i/o}$ isoforms that display enhanced tonic inhibition of AC activity, unlike the β_{3a}-AR that is confined to membrane rafts/caveolae.

To examine preferential $G\alpha_{i/o}$ coupling to the β_{3b}-AR, we performed [^{35}S]GTPγS immunoprecipitation to measure activation of specific $G\alpha$ subunits following receptor stimulation with CL316243. As these experiments must be done using membranes rather than whole cells, we first characterized the system by measuring cAMP responses. CL316243 stimulated cAMP accumulation in crude membranes prepared from CHO-β_{3a}-AR or CHO-β_{3b}-AR cells, albeit with lower potency than in whole cells (pEC_{50} β_{3a}-AR, 7.10 ± 0.26; β_{3b}-AR 7.29, ± 0.38; see Fig. 8, *A* and *B*). Maximum responses were reached only at 3 μM CL316243. When β_{3a}-AR or β_{3b}-AR membranes were treated with activated PTX, there was a substantial increase in basal cAMP, showing that in this experimental paradigm PTX does indeed remove tonic inhibition of adenylyl cyclase.

Nevertheless, the increase in CL316243-induced cAMP accumulation in β_{3a}-AR membranes was not significantly different with or without PTX pretreatment (Fig. 8*C*; E_{max} minus basal cAMP, control 1.66 ± 0.28 pmol/μg protein; PTX, 2.18 ± 0.30). In contrast, the membranes from β_{3b}-AR cells show not only the increased basal cAMP in the presence of PTX but also a significant increase in the maximal CL316243-induced cAMP response compared with untreated cells (Fig. 8*C*; E_{max} minus basal cAMP, control 1.72 ± 0.36 pmol/μg protein; PTX, 4.17 ± 0.50, $p < 0.001$). These experiments show that the distinct properties of β_3-AR isoforms seen in whole cells are recapitulated in crude membrane preparations. Furthermore, these data suggest that PTX not only removes tonic inhibition of adenylyl cyclase but also permits additional CL316243-stimulated cAMP accumulation via the β_{3b}-AR but not the β_{3a}-AR.

We then sought to verify that the increase in CL316243-stimulated cAMP following PTX pretreatment in β_{3b}-AR membranes was due to inhibition of receptor-$G\alpha_{i/o}$ coupling. We incubated membranes with GDP for 5 min at 30 °C, prior to addition of vehicle or 3 μM CL316243 and 1 nM [^{35}S]GTPγS for 20 min at 30 °C. Each $G\alpha$ subunit was immunoprecipitated with an isoform-selective antibody, and the bound [^{35}S]GTPγS was measured (Fig. 8, *D–H*). Both sets of membranes displayed activation of $G\alpha_s$, but the β_{3b}-AR membranes showed additional activation of $G\alpha_o$ that was sensitive to PTX treatment (Fig. 8*I*). These experiments indicate that the β_{3b}-AR, but not the β_{3a}-AR, is able to couple to $G\alpha_o$ and that inhibition of this coupling is associated with increased cAMP accumulation. We also found that BAT membranes displayed robust activation of $G\alpha_s$, but not any $G\alpha_{i/o}$ isoforms (Fig. 8, *D–H*), consistent with the cAMP studies done in whole brown adipocytes.

DISCUSSION

We show here that the β_{3b}-AR is able to couple to both $G\alpha_s$ and $G\alpha_o$, in agreement with the PTX sensitivity of CL316243-stimulated cAMP accumulation in whole cells and in crude membranes. In contrast, the β_{3a}-AR is unable to couple to $G\alpha_{i/o}$ in either native mouse brown adipocytes or recombinant CHO-K1 cells. Our previous study indicated that residues present in the unique β_{3a}-AR C-terminal tail may interfere with $G\alpha_{i/o}$ coupling due to interaction with other proteins such as caveolin (22). This notion was reinforced by the observation that the β_{3a}-AR C-terminal tail contains a motif that is similar to the caveolin interaction motif of many proteins ($\phi X\phi XXXX\phi$ or $\phi XXXX\phi XX\phi$ (23)). We investigated this idea by treating CHO-K1 cells expressing the β_3-AR isoforms with filipin III to disrupt membrane rafts or with a caveolin-1 siRNA and by examining the coupling of mutant β_{3a}-ARs. We have also demonstrated a direct association between the β_{3a}-AR and caveolin-1 using a proximity ligation assay, and we show that our findings in recombinant CHO-K1 cells are recapitulated in brown adipocytes derived from wild type or caveolin-1 knock-out mice.

CHO-K1 cells express caveolin-1 and exhibit caveolar structures (38–40). As knockdown of caveolin-1 in CHO-K1 cells promoted coupling of the β_{3a}-AR to $G\alpha_{i/o}$, we sought further evidence that caveolin-1 interacts with the receptor C-terminal tail. Our first step was to make a series of β_{3a}-ARs with mutations in single or multiple amino acids that might contribute to the caveolin-1 interaction. Single mutations of Phe-389 or Tyr-392 to alanine did not promote $G\alpha_{i/o}$ coupling of the β_{3a}-AR, whereas cAMP responses mediated by the combined mutants F389A,Y392A or F389A,Y392A, F398A became PTX-sensitive (Fig. 4). We also mutated Pro-384 to serine to mimic the rat β_3-AR sequence, as this receptor does couple to $G\alpha_{i/o}$ (34). Interestingly, both the P384S single mutant and a P384S,F389A double mutant showed PTX sensitivity, albeit slightly less than the other composite mutants. This study indicated that the motif P*XXXX*F*XX*Y is dominant in preventing $G\alpha_{i/o}$ coupling of the β_{3a}-AR, and it gave us the opportunity to test directly whether the mutants differed from the wild type receptor in their capacity to interact with caveolin-1. We examined this interaction using the Duolink *in situ* proximity ligation assay, which is based on close juxtaposition of antibodies directed against the two interacting partners (36). We were unable to perform this experiment with the β_{3b}-AR because the β_3-AR antibody is directed toward the β_{3a}-AR C-terminal tail. We did show, however, that the antibody detected the F389A,Y392A,F398A and the P384S,F389A mutants as well as the wild type β_{3a}-AR (Fig. 5*E*). The wild type receptor displayed robust interaction with caveolin-1 in this assay, whereas there was no signal in nontransfected CHO-K1 cells or in cells expressing the F389A,Y392A,F398A mutant. There was a very low signal in cells expressing the P384S,F389A β_{3a}-AR, suggesting that this receptor retained weak association with caveolin-1.

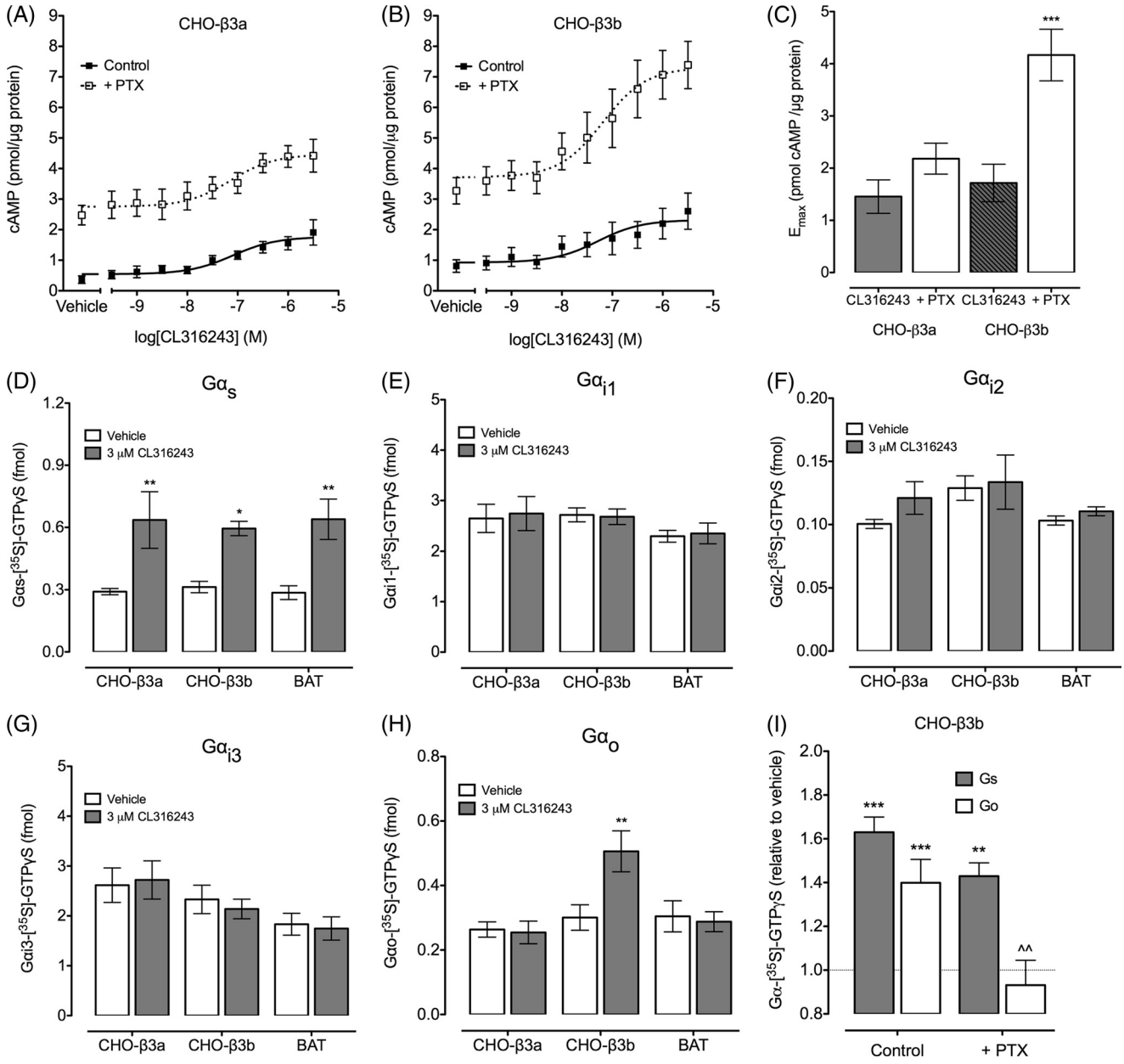

FIGURE 8. **Crude membranes isolated from CHO-K1 cells expressing the β_{3a}-AR or β_{3b}-AR display distinct receptor coupling and signaling.** Concentration-response curves were constructed for CL316243-stimulated cAMP accumulation by membranes prepared from CHO-β_{3a}-AR (*A*) or CHO-β_{3b}-AR cells (*B*). To test the effect of PTX, membranes were treated with activated PTX (20 μg/ml) for 15 min at room temperature. The data are expressed as pmol of cAMP/μg of protein, with no correction for basal cAMP levels. Values are means ± S.E. of 4–6 experiments (using independent crude membrane preparations) performed in triplicate. *C* shows the data from each concentration-response curve expressed as the maximal cAMP accumulation minus basal cAMP for membranes derived from CHO-β_{3a}- or CHO-β_{3b}-AR cells. Maximal CL316243-induced cAMP accumulation in β_{3a}-AR membranes was not significantly different with or without PTX treatment. In contrast, PTX-treated membranes from β_{3b}-AR cells show a significant increase in the maximal CL316243-induced cAMP response compared with untreated membranes ($p < 0.001$, one-way ANOVA with Newman Keuls multiple comparison test). [^{35}S]GTPγS immunoprecipitation was performed to assess direct activation of Gα_s (*D*), Gα_{i1} (*E*), Gα_{i2}, (*F*), Gα_{i3} (*G*), or Gα_o (*H*) following stimulation of the β_{3a}-AR (in CHO-K1 cells or BAT) or the β_{3b}-AR expressed in CHO-K1 cells. Reactions contained 100 fmol of [^{35}S]GTPγS in 100 μl. Data are expressed as femtomoles of [^{35}S]GTPγS; values are means ± S.E. of 4–6 experiments (using independent crude membrane preparations). 3 μM CL316243 stimulated a significant increase in Gα_s activation in all three membrane samples (**, $p < 0.01$; *, $p < 0.05$; two-way ANOVA with Bonferroni multiple comparison tests). The CHO-β_{3b}-AR membranes also displayed a significant increase in Gα_o activation (**, $p < 0.01$; two-way ANOVA with Bonferroni multiple comparison tests). *I*, pretreatment of β_{3b}-AR membranes with activated PTX abolished Gα_o activation but did not have a significant effect on Gα_s activation (***, $p < 0.001$; **, $p < 0.01$, response significantly different to vehicle; ^^, $p < 0.01$, CL316243 response in the presence of PTX significantly different from the CL316243 response in untreated membranes; two-way ANOVA with Bonferroni multiple comparison tests).

In combination with the functional properties of mutant receptors, the Duolink data indicate that an interaction with caveolin-1 does modulate the G protein coupling of the β_{3a}-AR.

The prototypical caveolin-binding motif consists of the sequences, $\phi X\phi XXXX\phi$, $\phi XXXX\phi XX\phi$, or a combination of the two (23). These consensus sequences were elucidated by screening phage display libraries using the caveolin scaffolding domain to select random peptide fragments. The most commonly occurring peptides were found to conform to one of the motifs above; however, there were many less abundant peptides

in which the spacing or number of aromatic residues varied from the consensus (23). Among proteins known to interact with caveolin, there are exceptions to the strict requirement for a consensus caveolin-binding motif with 3 or 4 aromatic residues. For example, the motif $\phi X\phi XXXX\phi XX\phi$ is present in $G\alpha_i$ and $G\alpha_o$ proteins, but the sequence of other G proteins known to interact with caveolin varies at one or more key positions; for example, $G\alpha_s$ has the sequence TKFQVDKVNFHMFDA, and $G\alpha_q$ has YFDLQSVIFRMVDA (23). Our data indicate that the β_{3a}-AR C terminus interacts with caveolin-1 despite lacking one of the consensus aromatic residues. More broadly, there may be many GPCRs that interact with the caveolin scaffolding domain of caveolin-1 despite lacking any cytoplasmic sequences that conform strictly to the $\phi X\phi XXXX\phi$ or $\phi XXXX\phi XX\phi$ consensus sites.

It has been pointed out that there is no single sorting signal that directs localization of GPCRs to membrane rafts (41). In addition, this localization may be unaffected, increased, or decreased by agonist treatment (3). For example, the δ-opioid receptor redistributes into raft domains upon agonist activation (42), possibly because the activated receptor adopts a longer conformation that has higher affinity for areas of the membrane bilayer such as rafts that are thickened due to enrichment with sphingomyelin (41). The α_{1A}-AR, on the other hand, colocalizes with raft markers both before and immediately after agonist stimulation, but it moves from membrane rafts within 3–10 min (43). Another study has shown that signaling by the β_2-AR is constrained by exclusion from cholesterol-rich raft nanodomains that are enriched in other components of the signaling machinery, including $G\alpha_s$ and AC (12). Increasing the abundance of liquid-ordered raft domains by increasing cholesterol content or overexpressing caveolin-3 inhibits β_2-AR-mediated cAMP responses, whereas disruption of rafts by cholesterol extraction with methyl-β-cyclodextrin increases both basal and maximal agonist-stimulated cAMP accumulation. Similar effects have been demonstrated in C6 glioma cells that express endogenous β_2-ARs, where disruption of membrane rafts with methyl-β-cyclodextrin or knockdown of caveolin-1/caveolin-2 by siRNA led to increased cAMP accumulation (44). Our Duolink proximity assay suggests that the β_{3a}-AR interacts with caveolin-1 in the absence of agonist, and in contrast to the β_2-AR studies, our functional data with filipin III indicate that signaling is more efficient in the presence of membrane rafts, both in CHO-K1 cells expressing the β_{3a}-AR and in brown adipocytes with endogenous receptors.

Chimeric $G\alpha_q/G\alpha_s$ and $G\alpha_q/G\alpha_i$ chimeras have been used as an alternative tool to test the coupling of mouse β_{3a}-AR and β_{3b}-AR isoforms (34). The Gα constructs consisted of $G\alpha_q$ with the C-terminal five amino acids that determine receptor coupling replaced by those from $G\alpha_s$ or $G\alpha_i$ (45, 46). This provides a single readout (increased intracellular Ca^{2+}) to measure the relative efficiency of coupling to $G\alpha_s$ and $G\alpha_i$ subunits. The β_{3a}-AR and β_{3b}-AR both coupled less efficiently to $G\alpha_i$ than to $G\alpha_s$, but there was no difference in the relative coupling of each isoform to $G\alpha_i$. This result is entirely consistent with our data, as we have also shown that there is no inherent difference in the capacity of the β_{3a}-AR and β_{3b}-AR to couple to $G\alpha_{i/o}$ (22). Instead, the difference between the two isoforms resides in their differential interaction with caveolin-1 and localization in membrane rafts/caveolae. In the study by Lenard *et al.* (34), membrane localization of the chimeric Gα subunits would be determined by the common $G\alpha_q$ component. It has been shown previously that $G\alpha_q$ interacts with caveolin-1 (47, 48) and is enriched in membrane raft fractions (49), although others have shown that the raft localization of $G\alpha_q$ is dependent on the extraction procedure used (43). Even if the $G\alpha_q$ chimeras were enriched in membrane rafts relative to bulk membrane, the high abundance of these proteins (34) would likely mask any differences in the $G\alpha_{q/i}$ coupling of the β_{3a}-AR and β_{3b}-AR isoforms.

In CHO-K1 cells, membrane rafts are enriched in $G\alpha_{i/o}$ and $G\alpha_s$ relative to the bulk membrane (50–52). The two predominant adenylyl cyclase isoforms expressed are AC6 and AC7 (53), with AC7 excluded from membrane rafts (54). In contrast, the AC6 isoform is enriched in membrane rafts, and this localization is known to be functionally important (12, 54, 55). We have shown that in CHO-K1 cells expressing the β_{3a}-AR, filipin treatment not only enhances PTX sensitivity but also causes a right shift of the concentration-response curve to CL316243. On the other hand, filipin treatment of cells expressing the β_{3b}-AR increases basal and maximal cAMP accumulation. In cardiomyocytes and S49 lymphoma cells expressing low levels of endogenous β-ARs, on the order of 30 fmol/mg protein, the molar ratio of receptor/$G\alpha_s$ protein/AC has been estimated as 1:100:3 (50). Our recombinant CHO-K1 cells have a 30-fold higher abundance of receptors, so AC6 is almost certainly the limiting step in cAMP accumulation, and the enrichment of AC6 in membrane rafts may be another key difference between β_{3a}-AR and β_{3b}-AR responses. In the presence of filipin, the β_{3a}-AR may display reduced responsiveness because it loses its co-localization with AC6, whereas the β_{3b}-AR becomes more responsive because the AC6 is redistributed throughout the membrane and has higher availability. Another key question is why the β_{3a}-AR does not couple to $G\alpha_{i/o}$ even though these subunits are also enriched in membrane rafts (51). We suggest that despite their close proximity within rafts, coupling may be suppressed because the activity of $G\alpha_{i/o}$ is inhibited by interaction with caveolin (56). In the presence of filipin, the β_{3a}-AR would not only lose co-localization with AC6 but also gain the ability to interact with $G\alpha_{i/o}$ that is no longer associated with caveolin.

We have shown that the effects of filipin III treatment or caveolin-1 knockdown observed in CHO-K1 cells expressing the β_{3a}-AR are seen also in cultured brown adipocytes. These cells express the β_3-AR at ~400 fmol/mg of protein (57–59). In untreated brown adipocytes, CL316243 potency is 10-fold lower than in CHO-K1 cells, despite only a 2.5-fold lower β_3-AR abundance, suggesting that the efficiency of cAMP generation is also decreased in the adipocytes. In CHO-β_{3a}-AR cells, filipin III treatment reduced the pEC_{50} of CL316243 without affecting the maximum response. In contrast, filipin III treatment of brown adipocytes had no effect on the pEC_{50} of CL316243, but the maximum cAMP response was reduced. This is consistent with the overall lower potency of CL316243 in adipocytes, evidence that a 10-fold higher receptor occupancy is required in adipocytes to achieve a maximum cAMP

response. When signaling efficiency is reduced further in the presence of filipin III, high concentrations of CL316243 cannot produce the same maximum response as that seen without filipin III. It has been shown that caveolin-1 knock-out mice have compromised cAMP accumulation in response to CL316243, due to composite effects on β_3-AR abundance and AC activity (18). Our data extend these findings by demonstrating that both filipin III treatment and knockdown of caveolin-1 in brown adipocytes cause cAMP responses to become PTX-sensitive, indicating that the β_{3a}-AR acquires coupling to $G\alpha_{i/o}$ proteins.

In conclusion, our study demonstrates that the β_{3a}-AR interacts with caveolin-1 and that the interaction affects functional coupling of the receptor to $G\alpha_{i/o}$ and $G\alpha_s$ subunits. Our work and that of others indicates that the reduced β_3-AR signaling in mice lacking caveolin-1 is due to disruption of a signaling complex containing caveolin-1, the β_{3a}-AR, $G\alpha_s$, and adenylyl cyclase and not just due to reduced β_3-AR abundance (16–18). Physiologically, the β_3-AR plays a major role in white and brown adipocytes, where caveolin-1 association serves to potentiate receptor-mediated cAMP accumulation and downstream responses such as lipolysis or thermogenesis. For other receptors such as the β_2-AR, raft localization and caveolin interaction undergo dynamic regulation due to requirements for strict spatial and temporal control of signaling (12). Thus, although membrane raft localization is a critical factor in organizing GPCR signaling complexes, the functional impact varies between receptors (41). Continuing studies on GPCRs will provide novel insights into the determinants that dictate association of receptors with caveolins, promote localization in membrane rafts, and thereby modulate receptor signaling.

Acknowledgments—We thank Dr. Debbie Thurmond for providing the caveolin-1 siRNA constructs and Dr. Robin Anderson (with permission from Dr. T. Kurzchalia) for the caveolin-$1^{+/+}$ and caveolin-$1^{-/-}$ mice.

REFERENCES

1. Simons, K., and Ikonen, E. (1997) Functional rafts in cell membranes. *Nature* **387,** 569–572
2. Sharma, P., Varma, R., Sarasij, R. C., Ira, Gousset, K., Krishnamoorthy, G., Rao, M., and Mayor, S. (2004) Nanoscale organization of multiple GPI-anchored proteins in living cell membranes. *Cell* **116,** 577–589
3. Patel, H. H., Murray, F., and Insel, P. A. (2008) G-protein-coupled receptor-signaling components in membrane raft and caveolae microdomains. *Handb. Exp. Pharmacol.* **186,** 167–184
4. Parton, R. G., and Simons, K. (2007) The multiple faces of caveolae. *Nat. Rev. Mol. Cell Biol.* **8,** 185–194
5. Hill, M. M., Bastiani, M., Luetterforst, R., Kirkham, M., Kirkham, A., Nixon, S. J., Walser, P., Abankwa, D., Oorschot, V. M., Martin, S., Hancock, J. F., and Parton, R. G. (2008) PDRF-Cavin, a conserved cytoplasmic protein required for caveola formation and function. *Cell* **132,** 113–124
6. Parton, R. G., Hanzal-Bayer, M., and Hancock, J. F. (2006) Biogenesis of caveolae. A structural model for caveolin-induced domain formation. *J. Cell Sci.* **119,** 787–796
7. Lajoie, P., Goetz, J. G., Dennis, J. W., and Nabi, I. R. (2009) Lattices, rafts, and scaffolds. Domain regulation of receptor signaling at the plasma membrane. *J. Cell Biol.* **185,** 381–385
8. Lajoie, P., Partridge, E. A., Guay, G., Goetz, J. G., Pawling, J., Lagana, A., Joshi, B., Dennis, J. W., and Nabi, I. R. (2007) Plasma membrane domain organization regulates EGFR signaling in tumor cells. *J. Cell Biol.* **179,** 341–356
9. Head, B. P., and Insel, P. A. (2007) Do caveolins regulate cells by actions outside of caveolae? *Trends Cell Biol.* **17,** 51–57
10. Xiang, Y., and Kobilka, B. (2003) The PDZ-binding motif of the β_2-adrenoceptor is essential for physiologic signaling and trafficking in cardiac myocytes. *Proc. Natl. Acad. Sci. U.S.A.* **100,** 10776–10781
11. Xiang, Y., Devic, E., and Kobilka, B. (2002) The PDZ-binding motif of the β_1-adrenergic receptor modulates receptor trafficking and signaling in cardiac myocytes. *J. Biol. Chem.* **277,** 33783–33790
12. Pontier, S. M., Percherancier, Y., Galandrin, S., Breit, A., Galés, C., and Bouvier, M. (2008) Cholesterol-dependent separation of the β_2-adrenergic receptor from its partners determines signaling efficacy: insight into nanoscale organization of signal transduction. *J. Biol. Chem.* **283,** 24659–24672
13. Balijepalli, R. C., Foell, J. D., Hall, D. D., Hell, J. W., and Kamp, T. J. (2006) Localization of cardiac L-type Ca^{2+} channels to a caveolar macromolecular signaling complex is required for β_2-adrenergic regulation. *Proc. Natl. Acad. Sci. U.S.A.* **103,** 7500–7505
14. Calaghan, S., and White, E. (2006) Caveolae modulate excitation-contraction coupling and β_2-adrenergic signaling in adult rat ventricular myocytes. *Cardiovasc. Res.* **69,** 816–824
15. Cohen, A. W., Razani, B., Schubert, W., Williams, T. M., Wang, X. B., Iyengar, P., Brasaemle, D. L., Scherer, P. E., and Lisanti, M. P. (2004) Role of caveolin-1 in the modulation of lipolysis and lipid droplet formation. *Diabetes* **53,** 1261–1270
16. Ahmad, F., Lindh, R., Tang, Y., Ruishalme, I., Ost, A., Sahachartsiri, B., Strålfors, P., Degerman, E., and Manganiello, V. C. (2009) Differential regulation of adipocyte PDE3B in distinct membrane compartments by insulin and the β_3-adrenergic receptor agonist CL316243. Effects of caveolin-1 knockdown on formation/maintenance of macromolecular signaling complexes. *Biochem. J.* **424,** 399–410
17. Cohen, A. W., Schubert, W., Brasaemle, D. L., Scherer, P. E., and Lisanti, M. P. (2005) Caveolin-1 expression is essential for proper nonshivering thermogenesis in brown adipose tissue. *Diabetes* **54,** 679–686
18. Mattsson, C. L., Andersson, E. R., and Nedergaard, J. (2010) Differential involvement of caveolin-1 in brown adipocyte signaling. Impaired β_3-adrenergic, but unaffected LPA, PDGF, and EGF receptor signaling. *Biochim. Biophys. Acta* **1803,** 983–989
19. Mattsson, C. L., Csikasz, R. I., Shabalina, I. G., Nedergaard, J., and Cannon, B. (2010) Caveolin-1-ablated mice survive in cold by nonshivering thermogenesis despite desensitized adrenergic responsiveness. *Am. J. Physiol. Endocrinol. Metab.* **299,** E374–E383
20. Evans, B. A., Papaioannou, M., Hamilton, S., and Summers, R. J. (1999) Alternative splicing generates two isoforms of the β_3-adrenoceptor which are differentially expressed in mouse tissues. *Br. J. Pharmacol.* **127,** 1525–1531
21. Hutchinson, D. S., Bengtsson, T., Evans, B. A., and Summers, R. J. (2002) Mouse β_{3a}- and β_{3b}-adrenoceptors expressed in Chinese hamster ovary cells display identical pharmacology but utilize distinct signaling pathways. *Br. J. Pharmacol.* **135,** 1903–1914
22. Sato, M., Hutchinson, D. S., Bengtsson, T., Floren, A., Langel, U., Horinouchi, T., Evans, B. A., and Summers, R. J. (2005) Functional domains of the mouse β_3-adrenoceptor associated with differential G protein coupling. *J. Pharmacol. Exp. Ther.* **315,** 1354–1361
23. Couet, J., Li, S., Okamoto, T., Ikezu, T., and Lisanti, M. P. (1997) Identification of peptide and protein ligands for the caveolin-scaffolding domain. Implications for the interaction of caveolin with caveolae-associated proteins. *J. Biol. Chem.* **272,** 6525–6533
24. Nevins, A. K., and Thurmond, D. C. (2006) Caveolin-1 functions as a novel Cdc42 guanine nucleotide dissociation inhibitor in pancreatic beta-cells. *J. Biol. Chem.* **281,** 18961–18972
25. Drab, M., Verkade, P., Elger, M., Kasper, M., Lohn, M., Lauterbach, B., Menne, J., Lindschau, C., Mende, F., Luft, F. C., Schedl, A., Haller, H., and Kurzchalia, T. V. (2001) Loss of caveolae, vascular dysfunction, and pulmonary defects in caveolin-1 gene-disrupted mice. *Science* **293,** 2449–2452
26. Néchad, M., Kuusela, P., Carneheim, C., Björntorp, P., Nedergaard, J., and Cannon, B. (1983) Development of brown fat cells in monolayer culture. I. Morphological and biochemical distinction from white fat cells in culture.

Exp. Cell Res. **149,** 105–118
27. Chernogubova, E., Hutchinson, D. S., Nedergaard, J., and Bengtsson, T. (2005) α_1- and β_1-adrenoceptor signaling fully compensates for β_3-adrenoceptor deficiency in brown adipocyte norepinephrine-stimulated glucose uptake. *Endocrinology* **146,** 2271–2284
28. Nevzorova, J., Bengtsson, T., Evans, B. A., and Summers, R. J. (2002) Characterization of the β-adrenoceptor subtype involved in mediation of glucose transport in L6 cells. *Br. J. Pharmacol.* **137,** 9–18
29. Tanishita, T., Shimizu, Y., Minokoshi, Y., and Shimazu, T. (1997) The β_3-adrenergic agonist BRL37344 increases glucose transport into L6 myocytes through a mechanism different from that of insulin. *J. Biochem.* **122,** 90–95
30. Kaslow, H. R., Lim, L. K., Moss, J., and Lesikar, D. D. (1987) Structure-activity analysis of the activation of pertussis toxin. *Biochemistry* **26,** 123–127
31. Moss, J., Stanley, S. J., Burns, D. L., Hsia, J. A., Yost, D. A., Myers, G. A., and Hewlett, E. L. (1983) Activation by thiol of the latent NAD glycohydrolase and ADP-ribosyltransferase activities of *Bordetella pertussis* toxin (islet-activating protein). *J. Biol. Chem.* **258,** 11879–11882
32. Halls, M. L., van der Westhuizen, E. T., Wade, J. D., Evans, B. A., Bathgate, R. A., and Summers, R. J. (2009) Relaxin family peptide receptor (RXFP1) coupling to $G\alpha_{i3}$ involves the C-terminal Arg-752 and localization within membrane Raft microdomains. *Mol. Pharmacol.* **75,** 415–428
33. Mistry, R., Dowling, M. R., and Challiss, R. A. (2011) [^{35}S]GTPγS binding as an index of total G-protein and Gα-subtype-specific activation by GPCRs. *Methods Mol. Biol.* **746,** 263–275
34. Lenard, N. R., Prpic, V., Adamson, A. W., Rogers, R. C., and Gettys, T. W. (2006) Differential coupling of β_{3A}- and β_{3B}-adrenergic receptors to endogenous and chimeric $G\alpha_s$ and $G\alpha_i$. *Am. J. Physiol. Endocrinol. Metab.* **291,** E704–E715
35. Hutchinson, D. S., Sato, M., Evans, B. A., Christopoulos, A., and Summers, R. J. (2005) Evidence for pleiotropic signaling at the mouse β_3-adrenoceptor revealed by SR59230A [3-(2-ethylphenoxy)-1-[(1*S*)-1,2,3,4-tetrahydronapth-1-ylamino]-2*S*-2-propanol oxalate]. *J. Pharmacol. Exp. Ther.* **312,** 1064–1074
36. Söderberg, O., Gullberg, M., Jarvius, M., Ridderstråle, K., Leuchowius, K. J., Jarvius, J., Wester, K., Hydbring, P., Bahram, F., Larsson, L. G., and Landegren, U. (2006) Direct observation of individual endogenous protein complexes in situ by proximity ligation. *Nat. Methods* **3,** 995–1000
37. Chernogubova, E., Cannon, B., and Bengtsson, T. (2004) Norepinephrine increases glucose transport in brown adipocytes via β_3-adrenoceptors through a cAMP, PKA, and PI 3-kinase-dependent pathway stimulating conventional and novel PKCs. *Endocrinology* **145,** 269–280
38. Abrami, L., Fivaz, M., Kobayashi, T., Kinoshita, T., Parton, R. G., and van der Goot, F. G. (2001) Cross-talk between caveolae and glycosylphosphatidylinositol-rich domains. *J. Biol. Chem.* **276,** 30729–30736
39. Zeng, Y., Tao, N., Chung, K. N., Heuser, J. E., and Lublin, D. M. (2003) Endocytosis of oxidized low density lipoprotein through scavenger receptor CD36 utilizes a lipid raft pathway that does not require caveolin-1. *J. Biol. Chem.* **278,** 45931–45936
40. Cheng, Z. J., Singh, R. D., Holicky, E. L., Wheatley, C. L., Marks, D. L., and Pagano, R. E. (2010) Co-regulation of caveolar and Cdc42-dependent fluid phase endocytosis by phosphocaveolin-1. *J. Biol. Chem.* **285,** 15119–15125
41. Bethani, I., Skånland, S. S., Dikic, I., and Acker-Palmer, A. (2010) Spatial organization of transmembrane receptor signaling. *EMBO J.* **29,** 2677–2688
42. Alves, I. D., Salamon, Z., Hruby, V. J., and Tollin, G. (2005) Ligand modulation of lateral segregation of a G-protein-coupled receptor into lipid microdomains in sphingomyelin/phosphatidylcholine solid-supported bilayers. *Biochemistry* **44,** 9168–9178
43. Morris, D. P., Lei, B., Wu, Y. X., Michelotti, G. A., and Schwinn, D. A. (2008) The α_{1a}-adrenergic receptor occupies membrane rafts with its G protein effectors but internalizes via clathrin-coated pits. *J. Biol. Chem.* **283,** 2973–2985
44. Allen, J. A., Yu, J. Z., Dave, R. H., Bhatnagar, A., Roth, B. L., and Rasenick, M. M. (2009) Caveolin-1 and lipid microdomains regulate G_s trafficking and attenuate G_s/adenylyl cyclase signaling. *Mol. Pharmacol.* **76,** 1082–1093
45. Conklin, B. R., Herzmark, P., Ishida, S., Voyno-Yasenetskaya, T. A., Sun, Y., Farfel, Z., and Bourne, H. R. (1996) C-terminal mutations of $G_q\alpha$ and $G_s\alpha$ that alter the fidelity of receptor activation. *Mol. Pharmacol.* **50,** 885–890
46. Coward, P., Chan, S. D., Wada, H. G., Humphries, G. M., and Conklin, B. R. (1999) Chimeric G proteins allow a high throughput signaling assay of G_i-coupled receptors. *Anal. Biochem.* **270,** 242–248
47. de Weerd, W. F., and Leeb-Lundberg, L. M. (1997) Bradykinin sequesters B2 bradykinin receptors and the receptor-coupled Gα subunits $G\alpha_q$ and $G\alpha_i$ in caveolae in DDT1 MF-2 smooth muscle cells. *J. Biol. Chem.* **272,** 17858–17866
48. Bhatnagar, A., Sheffler, D. J., Kroeze, W. K., Compton-Toth, B., and Roth, B. L. (2004) Caveolin-1 interacts with 5-HT2A serotonin receptors and profoundly modulates the signaling of selected $G\alpha_q$-coupled protein receptors. *J. Biol. Chem.* **279,** 34614–34623
49. Sugawara, Y., Nishii, H., Takahashi, T., Yamauchi, J., Mizuno, N., Tago, K., and Itoh, H. (2007) The lipid raft proteins flotillins/reggies interact with $G\alpha_q$ and are involved in G_q-mediated p38 mitogen-activated protein kinase activation through tyrosine kinase. *Cell. Signal.* **19,** 1301–1308
50. Ostrom, R. S., Post, S. R., and Insel, P. A. (2000) Stoichiometry and compartmentation in G protein-coupled receptor signaling: implications for therapeutic interventions involving G(s). *J. Pharmacol. Exp. Ther.* **294,** 407–412
51. Razani, B., Woodman, S. E., and Lisanti, M. P. (2002) Caveolae. From cell biology to animal physiology. *Pharmacol. Rev.* **54,** 431–467
52. Head, B. P., Patel, H. H., Roth, D. M., Murray, F., Swaney, J. S., Niesman, I. R., Farquhar, M. G., and Insel, P. A. (2006) Microtubules and actin microfilaments regulate lipid raft/caveolae localization of adenylyl cyclase signaling components. *J. Biol. Chem.* **281,** 26391–26399
53. Varga, E. V., Stropova, D., Rubenzik, M., Wang, M., Landsman, R. S., Roeske, W. R., and Yamamura, H. I. (1998) Identification of adenylyl cyclase isoenzymes in CHO and B82 cells. *Eur. J. Pharmacol.* **348,** R1–R2
54. Crossthwaite, A. J., Seebacher, T., Masada, N., Ciruela, A., Dufraux, K., Schultz, J. E., and Cooper, D. M. (2005) The cytosolic domains of Ca^{2+}-sensitive adenylyl cyclases dictate their targeting to plasma membrane lipid rafts. *J. Biol. Chem.* **280,** 6380–6391
55. Thangavel, M., Liu, X., Sun, S. Q., Kaminsky, J., and Ostrom, R. S. (2009) The C1 and C2 domains target human type 6 adenylyl cyclase to lipid rafts and caveolae. *Cell. Signal.* **21,** 301–308
56. Xu, W., Yoon, S. I., Huang, P., Wang, Y., Chen, C., Chong, P. L., and Liu-Chen, L. Y. (2006) Localization of the κ-opioid receptor in lipid rafts. *J. Pharmacol. Exp. Ther.* **317,** 1295–1306
57. Sillence, M. N., Moore, N. G., Pegg, G. G., and Lindsay, D. B. (1993) Ligand binding properties of putative β_3-adrenoceptors compared in brown adipose tissue and in skeletal muscle membranes. *Br. J. Pharmacol.* **109,** 1157–1163
58. Adli, H., Bazin, R., Vassy, R., and Perret, G. Y. (1997) Effects of triiodothyronine administration on the adenylyl cyclase system in brown adipose tissue of rat. *Am. J. Physiol.* **273,** E247–E253
59. Malo, A., and Puerta, M. (2001) Oestradiol and progesterone change β_3-adrenergic receptor affinity and density in brown adipocytes. *Eur. J. Endocrinol.* **145,** 87–91